TOPICAL REVIEW

Breast Cancer Detection Using Mammography: Image Processing to Deep Learning

SHAHZAD AHMAD QURESHI[1,2], **AZIZ-UL-REHMAN**[3,4], **LAL HUSSAIN**[5,6],
TOUSEEF SADIQ[7], **(Member, IEEE), SYED TAIMOOR HUSSAIN SHAH**[8],
ADIL ASLAM MIR[5], **MUHAMMAD AMIN NADIM**[9,10], **DARNELL K. ADRIAN WILLIAMS**[11],
TIM Q. DUONG[11], **QURAT-UL-AIN CHAUDHARY**[1], **NATASHA HABIB**[12], **ASRAR AHMAD**[13],
AND SYED ADIL HUSSAIN SHAH[14]

[1]Department of Computer and Information Sciences, Pakistan Institute of Engineering and Applied Sciences (PIEAS), Islamabad 45650, Pakistan
[2]Centre for Mathematical Sciences, Pakistan Institute of Engineering and Applied Sciences (PIEAS), Islamabad 45650, Pakistan
[3]Department of Physics and Astronomy, Macquarie University, Sydney, NSW 2109, Australia
[4]Agriculture and Biophotonics Division, National Institute of Lasers and Optronics College, Pakistan Institute of Engineering and Applied Sciences (PIEAS), Islamabad 45650, Pakistan
[5]Department of Computer Science and Information Technology, King Abdullah Campus, The University of Azad Jammu and Kashmir, Muzaffarabad, Azad Kashmir 13100, Pakistan
[6]Department of Computer Science and Information Technology, Neelum Campus, The University of Azad Jammu and Kashmir, Athmuqam, Azad Kashmir 13230, Pakistan
[7]Centre for Artificial Intelligence Research (CAIR), Department of Information and Communication Technology, University of Agder, 4879 Grimstad, Norway
[8]PolitoBIOMed Laboratory, Department of Mechanical and Aerospace Engineering, Politecnico di Torino, 10129 Turin, Italy
[9]Learning Sciences and Digital Technologies, Università Telematica Pegaso, 80143 Naples, Italy
[10]Learning Sciences and Digital Technologies, Università degli Studi di Foggia, 71122 Foggia, Italy
[11]Department of Radiology, Albert Einstein College of Medicine, Bronx, NY 10461, USA
[12]Department of Physics and Applied Mathematics, Pakistan Institute of Engineering and Applied Sciences (PIEAS), Islamabad 45650, Pakistan
[13]Department of Medical Sciences, Pakistan Institute of Engineering and Applied Sciences (PIEAS), Islamabad 45650, Pakistan
[14]Department of Research and Development (R&D), GPI SpA, 38123 Trento, Italy

Corresponding authors: Touseef Sadiq (touseef.sadiq@uia.no) and Shahzad Ahmad Qureshi (drsaqureshi@pieas.edu.pk)

ABSTRACT Breast cancer stands as a predominant health concern for women globally. As mammography is the primary screening tool for breast cancer detection, improving the detection of breast cancer at screening could save more lives. This mammography review paper comprehensively reviews computer-aided techniques during a specific time frame for the segmentation and classification of microcalcification, evaluating image processing, machine learning, and deep learning techniques. The review is meticulously carried out, adhering closely to the Preferred Reporting Items for Systematic Reviews and Meta-Analyses (PRISMA) guidelines. This article focuses on mammographic breast cancer detection approaches based on automated systems, discussed chronologically from 1970 through 2023. This article encompasses the breadth of artificial intelligence-based methods from the most primitive to the most sophisticated models. Image processing and machine learning-based methods are comprehensively reviewed. Evaluating a deep learning architecture based on self-extracted features for classification tasks demonstrated outstanding performance. Large-scale datasets required for a broader and in-depth analysis of novel methods for breast cancer detection are also discussed in this article. This research work is aligned with the United Nations' sustainability development goals.

INDEX TERMS Breast cancer, mammography, microcalcification, deep learning, convolution neural networks, machine learning.

The associate editor coordinating the review of this manuscript and approving it for publication was Md. Moinul Hossain.

I. INTRODUCTION

Globally, breast cancer ranks as the most prevalent cancer and holds the second-highest mortality rate among women internationally. According to the WHO, half a million women

worldwide die each year from breast cancer [1]. In 2018, breast cancer claimed the lives of 627,000 women, making up 15% of all cancer-related deaths. In Europe, there were 3.9 million new cases reported in 2018 accounting for 25% of the world's cancer toll [2]. This research reviews breast cancer detection through mammography over some time, aligning with several UN Sustainable Development Goals (UDGs) [3] by improving early detection (goal 3), optimal health and well-being (goal 5), contributing to industry, innovation, and infrastructure through technological innovation and collaboration (goal 9) and fostering partnerships for collective action (goal 17).

Statistically, the increase in the death rate from breast cancer can be attenuated by adopting routine screening procedures at its early stages. A reliable technique for breast cancer screening is mammography. A mammogram can often reveal breast changes that could represent cancer years before physical symptoms develop. The goal of screening programs such as yearly mammography is to promote early cancer detection while the cancer is still clinically occult. Ductal carcinoma in situ (DCIS) is the earliest form of breast cancer, as it is confined to the ductal system and is not yet invasive. Over 90% of non-palpable DCIS is detected by microcalcifications alone [4]. Therefore, differentiating benign from malignant calcifications based on their radiographic appearance is very important [5]. Due to their small size (0.1-1.0 mm) and lack of background contrast on images, malignant calcifications have the potential to be difficult to observe and characterize [6]. Accurately identifying and classifying such calcifications on screening mammograms can be challenging. Previous computer-aided detection (CAD) systems were disappointing, yielding reduced accuracy, increased biopsies, and no definite improvement in cancer detection rate [7].

Optimizing the ability to differentiate benign from malignant calcifications is an area of great interest in Artificial Intelligence (AI) through Deep Learning (DL) [8]. DCIS often has a natural history of non-progression, with an estimated up to about 40% progressing to invasive carcinoma, according to some investigators [9]. Others have estimated the progression of DCIS to invasive cancer to be about 53% [10]. As DCIS is a pre-invasive and a non-obligate precursor to invasive carcinoma, with approximately half of the cases remaining non-invasive, greater emphasis is placed on detecting early invasive breast cancer. While there are many potential mammographic features associated with invasive breast cancer at screening mammography, the most common mammographic appearance is that of a mass [11]. The goal of mammography in detecting invasive breast cancer is early detection when it is 1 cm or smaller, with a 95% chance of 10-year survival compared to 85% and 60% survival at 1-2 cm and 2-5 cm, respectively [12]. Morphological features describing a mammographic mass's shape and margins help differentiate benign from malignant masses. These features have been exploited in DL using CNN for shape classification, yielding an accuracy of 80% on a public dataset [13].

Mammography uses low-dose X-rays to approximate the distribution of absorption coefficients depicted on imaging as structural density variation, revealing anatomy based on radiomic features used to translate/detect the presence of breast cancer. In this context, this review article uses large publicly available X-ray mammography datasets from different time frames to perform a detailed summary of breast cancer diagnosis methodology. Although previous studies have examined similar literature, most cover a specific range. They must be revised to examine a broad spectrum of methodologies over a considerable period. Examining the consistent improvements in technology and image quality can provide a better understanding of how best to detect and classify lesions with greater accuracy and efficiency.

Analyzing a mass manually is a time-intensive task, with the effectiveness of contrast enhancement during screening relying on both image quality and the radiologist's skill level. Screening techniques that are used include clinical and self-examination (CSE) of the breast, mammography, breast ultrasound, and magnetic resonance imaging (MRI) [1]. CSE is a good approach where limited clinical resources are available with high sensitivity (60-70%) and specificity (90-97%) [14], [15]. Among US women, mammography screening has reduced mortality [16]. Although it has a positive impact, screening mammography has many false positives [17]. In addition, CSE performance varies based on the physician's experience and knowledge. This issue can be resolved with multiple clinical exams, but this approach is costly, arduous, and time-consuming.

Since 1990, researchers developed CAD tools to improve screening accuracy. While computer-aided mammography (CAM) has been in use for over two decades, the automatic detection of microcalcification still needs to be improved, mainly due to its low contrast, fuzzy nature, and poor discrimination from the contiguous pixels. Researchers have been using a variety of algorithms for the automatic diagnosis of microcalcification. Different techniques and methods are used for feature extraction and enhancement, such as wavelet transforms, segmentation, and clustering. The medical community is successfully applying advanced AI machine learning (ML) techniques, to improve accuracy in cancer screening procedures [18]. In this context, unsupervised learning methods have successfully aided radiologists in improving screening outcomes [19], [20], [21], [22], [23], [24]. ML techniques have allowed for the detailed analysis of mammography images to be performed using feature extraction techniques like textural, statistical, and sub-band transformation, in addition to other traditional feature extraction techniques. These features tune classical ML techniques to classify unknown images into benign and malignant cases.

Jeyasingh and Veluchamy [25] proposed a Modified Bat Algorithm (MBA) for feature selection to enhance

the accuracy of breast cancer diagnosis. By eliminating irrelevant features from the WDBC, MBA improves the performance of Random Forest (RF) classification, yielding better results in various evaluation metrics. This research demonstrates the effectiveness of an MBA in improving diagnostic accuracy, highlighting its potential to streamline breast cancer diagnosis. Mahesh et al. [26] introduced a novel ensemble learning approach combining five ML models: Support Vector Machine (SVM), k-Nearest Neighbor (k-NN), Decision Tree (DT), RF, and Logistic Regression (LR) for breast cancer prediction, achieving 98.14% accuracy, enabling early detection and effective treatment. In another work, Zhou et al. [27] proposed an ML-based diagnostic system for breast cancer that achieves 99.12% accuracy using the AdaBoost-Logistic algorithm on the Wisconsin breast cancer dataset, demonstrating the potential for improved early detection and treatment. Islam et al. [28] used ML and Explainable AI to enhance breast cancer diagnosis accuracy. This study compares five ML algorithms, viz. DT, RF, LR, Naive Bayes (NB), and XGBoost on a dataset of 500 patients, with XGBoost achieving 97% accuracy. SHAP analysis provided feature-level insights, improving model interpretability and trustworthiness. Ünalan et al. [29] conducted a comparative study of ML algorithms and ensemble methods to enhance breast cancer classification accuracy. LGBM achieved 98.9% accuracy, while ensemble methods reached 99.5%. This study identifies crucial features and highlights the importance of en-semble learning and cross-validation for distinguishing malignant from benign cases.

In 2017, Abdelhafiz et al. published a review of 83 studies applying CNNs to mammography. Their review spanned a period of 1995 to 2017 and DL techniques for lesion localization and detection, risk assessment, image retrieval, high resolution reconstruction, and classification tasks. Both public and private datasets were included [30]. In 2019, Gardezi et al. reviewed DL techniques for mammogram datasets spanning a 5-year period, which discussed breast density estimation, mass detection, and mass classification, demonstrating how DL can contribute to the diagnostic performance of CAD systems [31]. In 2019, Geras et al. performed a review comparing conventional CAD, which uses prompts to demonstrate possible cancers, to AI-based CAD. Their review discusses the advantages of CAD system, which include fewer false positives and sensitivity equal to radiologists, allowing its use as a double reader and potentially as an independent first reader in the dismissal of normal cases [32]. More recently, Hickman et al. [33] published a meta-analysis of 15 studies in 2023 amal-gamating 185252 cases read by ML algorithms versus human readers. The overall area under the curve for the receiver operating characteristic AUC (ROC) curve for ML was 0.89, and for the human readers was 0.85. They concluded that ML algorithms as stand-alone applications in screening mammography can exceed the performance of human readers in detecting breast cancer and enhance

efficiency. Similarly, in a recent work, Khan et al. [34] carried out a review of representation learning-based methods using whole-breast MRI scans without expert radiologists' help to predict pathological complete response to neoadjuvant chemotherapy (NAC) in breast cancer. The immediate effects included reducing the toxicity of unnecessary NAC, with improved clinical outcomes.

Our review is on breast cancer diagnosis and detection in mammography from 1970 to 2023. We focused on the evolution of techniques over this period chronologically, including image preprocessing and enhancement methods, feature extraction methods with ML, and DL methods applied to mammography datasets. The value of this presentation is that it is oriented to professionals in the computing segment of healthcare, reaching beyond radiologists and clinicians. The main contributions of this article are:

- This work encompasses mammography based on early diagnosis and breast cancer detection, high-lighting the significant achievements from 1970 to 2023 using three keywords, namely (mammography AND microcalcification AND breast cancer).
- The notion is to divide the work into three main basic strategies for early breast cancer detection: Image Processing (IP)-based techniques, ML-based solutions, and DL algorithms.
- Competing algorithms have been briefly discussed in the field of mammography.
- All datasets of mammography have been discussed.
- Recent state-of-the-art techniques have been compared and discussed.

This review is conducted carefully, following the preferred reporting items for Systematic Reviews and Meta-Analyses (PRISMA) guidelines. The PRISMA flow diagram illustrat-ing the salient steps of the electronic literature collection process is shown in Figure 1. The search was carried out in 20, 16, 10, and 8-year intervals based on the keywords illustrated in Table 1. These intervals enable a comprehensive overview of the field's evolution, highlighting progress, and identifying areas for further investigation.

The time intervals (20, 16, 10, and 8 years) were chosen to reflect significant milestones and advancements in breast cancer research and treatment. The divisions allow for an examination of former trends and shifts in research focus (20 years), medium-term developments and establishment of current standards (16 years), recent advancements and emerging trends (10 years) and very recent studies and cutting-edge research (8 years). The last column shows the highest-citation articles in different periods for manual and computer-aided techniques. The compilation and analysis of mammography data involved an extensive online search of published literature from the Macquarie University library. The electronic bibliographic databases that have been used include Macquarie University library, Semantic Scholar, PubMed, Google Scholar, the Biological Science database, Springer Journals Complete-Open Access, the SciTech Pre-mium Collection, Taylor & Francis Open Access, the Catalog
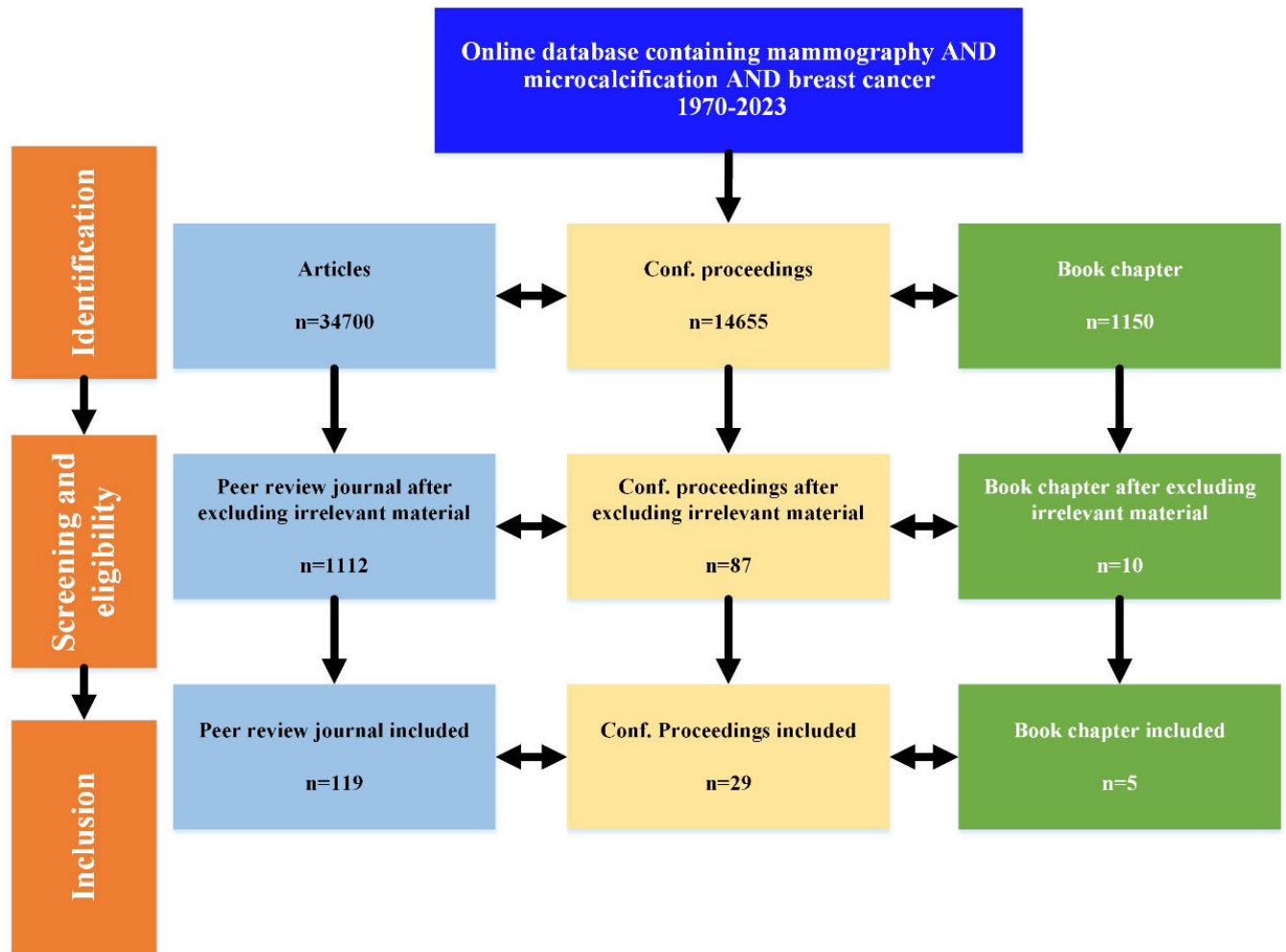
FIGURE 1. The PRISMA flow chart (1970-2023) from manual, ML and DL methods depicting the online research literature.

of Open Access Journals, Wiley-Blackwell Open Access Titles, the Engineering Database, Wiley Open Content, the Computer Science Database, and IEEE Open Access Journals and Conferences. The authors conducted the literature search, with subsequent reviewers independently assessing the article's relevance based on their titles and abstracts relevant to the study or scope of the review paper, and suitability of the methodology for the review article. The three main themes, manual-aided, ML, and DL are equally crucial for the early diagnosis problem. Also, the manual-aided articles (conventional IP techniques) were the most cited due to their relatively longer presence in re-search databases. The converse is true for DL-based articles, which are more recent and have needed more time to accrue citations. We have concisely reviewed primitive to recent methodologies and techniques, including novel DL architectures-based ideas and approaches related to mammography for micro-calcification detection in the breast.

II. MATERIAL AND METHODS

This study highlights explicitly the techniques used to detect abnormalities in breast cancer mammograms spanning 1970-2023 to provide researchers with a quick overview of employed methods. A basic breast image classification scheme is illustrated in Figure 2. We discussed the methods to detect breast cancer via mammography using (a) image preprocessing methods, including image enhancement methods, (b) different feature extraction methods with ML approaches, and (c) DL-based convolutional neural network (CNN) methods using three approaches, namely novel CNN algorithms, transfer learning, where pre-trained models are fine-tuned for mammography analysis, and DL-based feature extraction, which can be used as input for traditional ML classifiers. These methods are applied to different breast mammography datasets.

A. PREPROCESSING

Preprocessing is a complex task that involves missing values, transforming, and preparing the mammographic dataset for further analysis. The common reasons for missing values in mammography data are patient information not recorded, image acquisition faults, and failure to feature detection. The missing values can appear in various forms, depending on the specific data collection process and variables being

TABLE 1. Top citation methods for the evolution of mammography from 1970-2023 based on the defined slabs (MA stands for Manual Aided, and CA stands for Computer-Aided).

Years slab	Methods	Specific Type Basis	Description	Refs.	No. of citations
1970-1989 (20)	MA	IP	Mass screening through modern mammography.	[35]	699+
	CA	ML	Radiographic appearance of the breast parenchyma-based detection.	[36]	376+
1990-2005 (16)	MA	IP	Role of hormone replacement therapy correlated with age and micro-calcification density.	[37]	1509+
	CA	ML	Four methods for surveillance of mutation carriers due to BRCA1 and BRCA2 mutation.	[38]	1498+
		DL	Novelty detection for identification of mass mammograms.	[39]	483+
2006-2015 (10)	MA	IP	Breast screening with MRI as an adjunct to mammography.	[40]	3469+
	CA	ML	Diagnosing mammographic masses using scalable image retrieval and scale-invariant feature transform (SIFT).	[41]	146+
		DL	A swarm intelligence optimized wavelet neural network method for breast cancer detection.	[42]	477+
2016-2023 (8)	MA	IP	Tumor size, over-diagnosis and mammography effectiveness.	[43]	727+
	CA	ML	Breast mass classification based on SVM and Extreme Learning Machine (ELM).	[44]	183+
		DL	Detection of radiological lesions in mammograms using DL.	[23]	1071+

measured. Some common examples of missing values are Not a Number (NaN) which may represent missing or invalid values for continuous variables like pixel intensity or breast cancer size. The empty or blank fields indicate missing information for categorical variables like breast density or lesion location. It's essential to identify and handle missing values appropriately to ensure accurate analysis and interpretation of mammography data.

The preprocessing steps help prepare mammography data for effective ML and DL model training, improving the accuracy and reliability of image analysis and diagnosis. The most commonly used techniques are image resizing to a consistent size and normalizing to a common range [0, 1] to facilitate model training. Standardizing image intensity and size to facilitate comparison is essential across different images and datasets. Moreover, removing noise and artifacts is important from mammograms to improve quality and reduce potential biases. The identification of regions of interest (ROIs), such as tumorous areas plays a key role. To increase diversity and reduce overfitting, data augmentation of mammograms is also carried out through transformations like rotation, flipping, and scaling.

B. IMAGE PROCESSING METHODS

Mammographic images, whether analyzed through self-examination or intelligent algorithms, can be challenging to interpret. The focus is primarily on the contrast between malignant and normal tissues, with tumors or microcalcifications appearing as white or dense regions. Enhancing these images to detect microcalcification involves a range of direct and indirect techniques. The complexity of this task is underscored by the following challenges: Direct image enhancement means improving the perceptual quality of the image by establishing correct discriminative contrast using direct techniques. Rangayyan et al. [45] suggested the adaptive neighborhood technique, in which the local contrast of an image is computed. Tang et al. [46] proposed a technique called multiscale local contrast, which decomposes

contrast using a wavelet domain, improving contrast details in different scales.

In the indirect contrast enhancement technique, the image histogram is modified instead of directly manipulating the image contrast. The most popular indirect image contrast enhancement techniques are based on histogram modeling. Significant variants of this technique are: In the histogram equalization (HE) technique, grey levels are distributed equally in the output, whereas input image mapping is proportional to the cumulative intensity [47]. This technique enhances the contrast of images globally, and the abnormal regions are filled close to contrast values. Therefore, an increase in the lower local contrast rises to higher contrast levels, and unnatural artifacts are seen in the output image. An adaptive histogram computes the difference in histograms against distinct regions of an input image. Multiple histograms are used to reallocate the contrast values of an image so that local contrast and edges can be enhanced in each region. In the adaptive and contrast limited adaptive histogram equalization (ACLAHE), an image's enhancement amount is equalized by computing the histogram of sub-matrices and truncated to limit the enhancement gray levels [48]. In the minimum mean brightness error bi-histogram equalization (MMBEBHE) technique, the image is divided into two parts depending on a threshold value. The threshold is calculated by finding all possible separated ranges of intensity values in an image and then finding the Absolute Mean Brightness Error (AMBE) followed by HE. In the case of an inhomogeneous background of a mammogram, local-based enhancement techniques can perform better. Such a popular technique is fixed-neighborhood statistical enhancement [49]. It estimates the background of an input image by computing the statistical properties of a pixel in the neighborhood and suppresses the estimated background. As a result, an increase in the local contrast of an image occurs.

Recently, novice image processing methods with DL have been adopted in diverse fields that can be involved in early breast cancer detection and classification. Sofos et al. [50], [51], [52] presented a lightweight DL model for
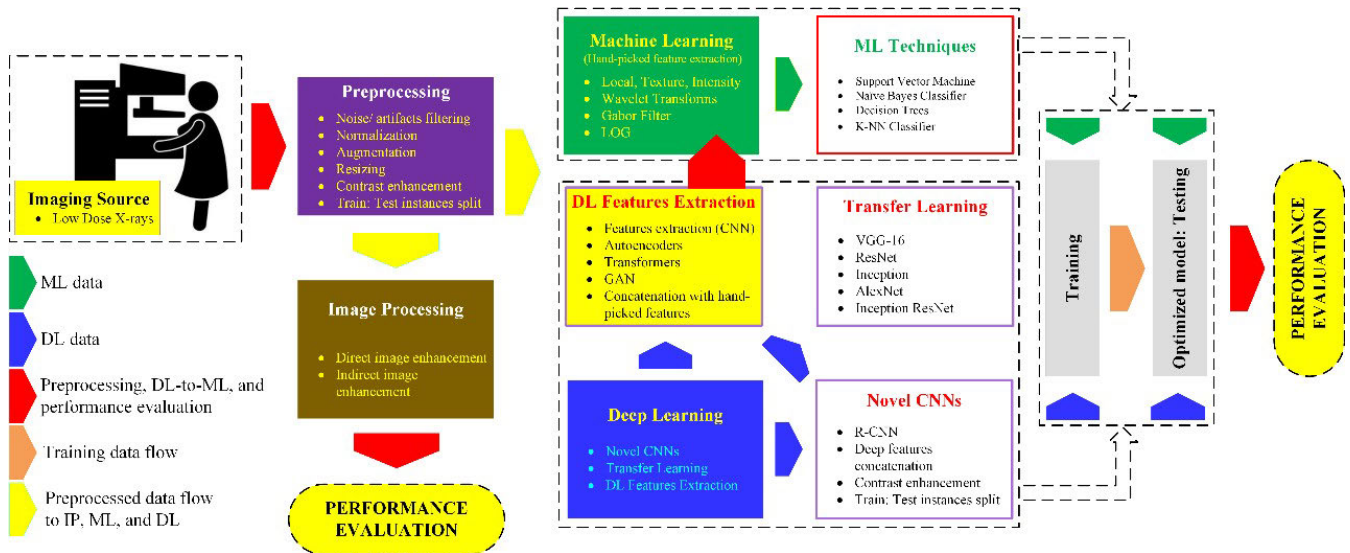
FIGURE 2. Breast cancer detection techniques based on mammography. The data flow is depicted by the arrows, initiating with the ingestion of the dataset, followed by a crucial pre-processing stage that feeds into three parallel strategies. The IP pipeline is applied for performance evaluation, whereas the ML and DL branches undergo training and testing phases before performance analysis. In the ML branch, feature extraction is facilitated through either manual feature engineering or DL-based feature extraction, or a fusion of both types of static and dynamic features. Conversely, the DL branch employs novel CNN architectures, TL, and automatic feature extraction, to supply features to the ML branch.

reconstructing high-resolution turbulent flow images from low-resolution, noisy data. Achieving a state-of-the-art PSNR of 45, this approach offers a faster alternative to traditional simulation methods for fluid dynamics applications with limited and noisy data. Poulinakis et al. [53] investigated the effectiveness of ML methods versus cubic splines in interpolating sparse and noisy experimental data. The findings highlight the strengths of each approach, providing valuable insights for accurate signal interpolation in scientific simulations and laboratory experiments. Furthermore, Sofos et al. [54] explored CNN for reconstructing compressible turbulent flow fields. A parallel framework upscales coarse data to fine-resolution images using an encoder-decoder network with residual and skip connections.

C. CLASSIFICATION

Feature extraction in clinical images is an important pre-processing step for ML and DL algorithms. It helps reduce redundant data and an algorithm's learning time. This section highlights feature extraction methods, followed by a brief overview of some of the most prominent methods proposed in the past.

1) FEATURE EXTRACTION FOR ML

Feature extraction reduces the dataset's dimensionality by condensing it into smaller subsets for processing. An undesirable effect of a large dataset is the buildup of many variables, requiring much computational power. Various feature extraction methods are illustrated in Figure 3. A brief overview of each of these methods follows next. Several researchers suggested that different local features in mammographic images can be extracted for classification.

Zhang et al. [55] divided local mammogram features into two classes, i.e., spatial (average and standard deviation intensities of foreground and background) and morphological features (moment, compactness, and Fourier descriptor). Spatial, morphology, and cluster description features were used to designate mammogram clusters. Davies et al. [56] proposed a technique using a few local mammographic features (mean intensity level, area, the ratio based on the area to the squared maximum-linear dimension, the strength of edge, and shape parameter).

- Textual Feature Extraction: Textural features are repeated or identical arrangements of patterns of pixels' intensities that refer to characteristics of an object, such as its appearance, shape, size, density, coarseness, and contrast. Different techniques for extracting texture-based features are the surrounding region dependence method (SRDM) [57], spatial gray-level dependence method (SGLDM) [58], gray-level run-length method (GLRLM) [59], and gray-level difference method (GLDM) [60].

- Intensity-based Feature Extraction: It consists of first-order statistics using features like mean, mode, variance, and standard deviation to find the intensity and its variation [61]. Here, a large set of sampling features can be extracted from a pixel's local neighborhood to train learning algorithms. However, the spatial arrangement of a pixel, a key factor for detecting and classifying abnormal tissues in mammograms, needs to be considered.

- Multi-scale Feature Extraction: The disadvantage of using texture-based features is that all methods focus on the single scale of a pixel. To extract features, Laws [62]
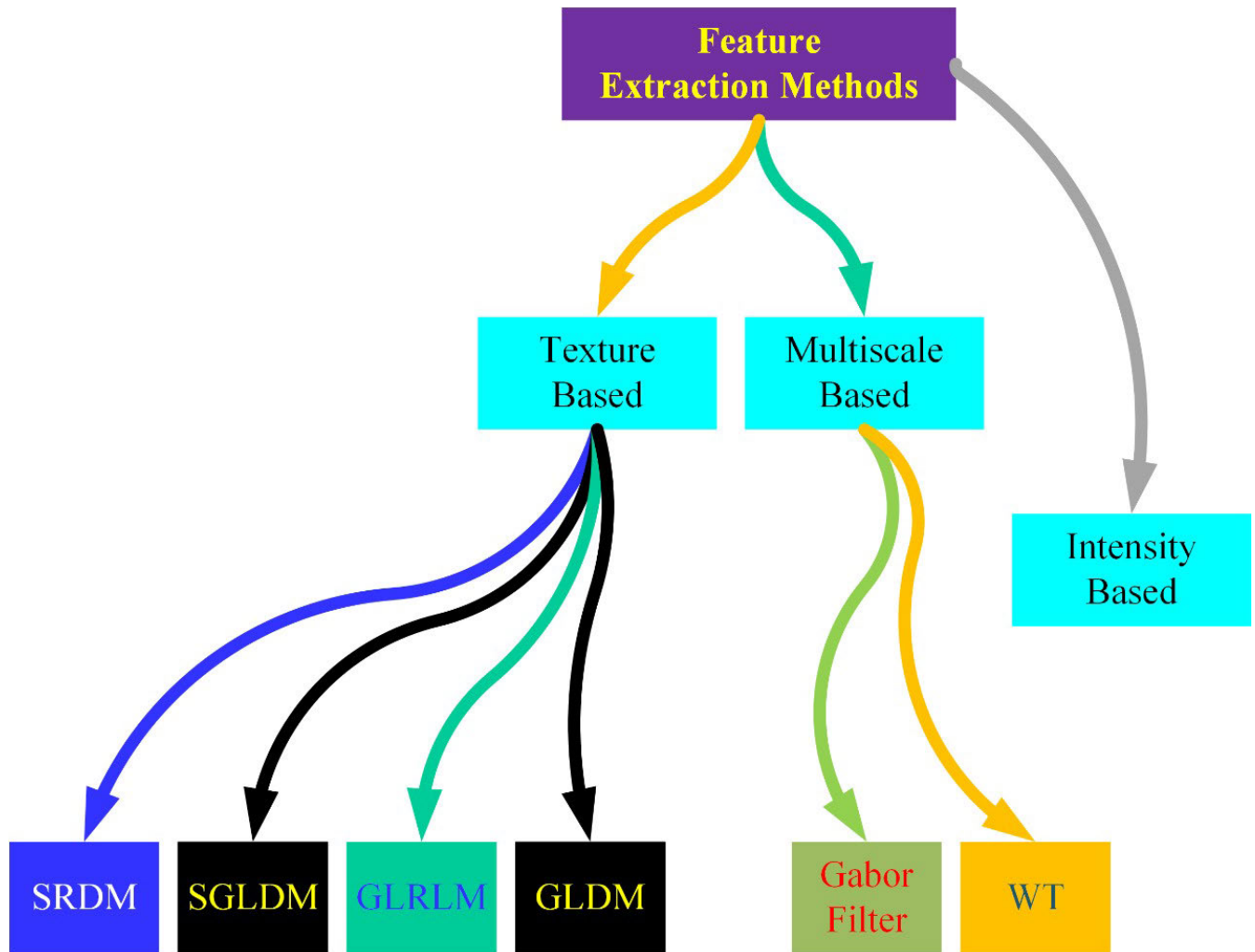
FIGURE 3. Well-known feature extraction methods and their classification, where SRDM represents Surrounding Region Dependence Method, SGLDM is Spatial Gray Level Dependence Matrix, GLRLM symbolizes Gray-Level Run-Length Matrix, GLDM depicts Gray-Level Difference Matrix, and WT are the wavelet transform-based features.

has explained a system in which linear transformation and energy computation perform better than the texture features of second-order statistics. Over time, many researchers have proposed improved methods for better performance by domain transformation, like wavelet transform-based methods [62], [63], [64], [65], Gabor Filter Bank Methods [66], and Laplacian of Gaussian Method [67].

2) ML APPROACHES

Extracting the most discriminative feature set is an essential factor in classification [68]. The latest ML algorithms can detect and classify normal and cancerous tissues (benign or malignant). A brief overview of important classifiers is given by:

- k-Nearest Neighbor (k-NN) Classifier: Alpaslan et al. [69] developed a decision support system to aid experts in analyzing mammogram images for breast cancer detection. The system involves preprocessing

mammogram images to enhance clarity, segmenting the mass, extracting features from the tumor mass, and classifying the mass as normal, benign, or malignant using k-NN classifiers, to assist in accurate breast cancer diagnosis. It is used to categorize benign, malignant, and normal tissues. It finds the distance between unobserved data and all the known data in k-classes, and the unknown instance is given the class name depending on the shortest distance from the known data classes. The Minkowski distance, dM, is a generalized form for the Euclidean- (L1-norm) and the Manhattan-(L2-norm) distances that are used with the k-NN classifier, as given by:

$$d_M = \left(\sum_{i=k}^{k} |x_i - y_i|^q \right)^{\frac{1}{q}} \quad (1)$$

The number of features is k, for object x the value of feature is x_i whereas for object y the value of feature is

y_i. The value of q defines the Manhattan and Euclidean metrics as one and two respectively.

- Decision Tree Classifier: Kamalakannan and Babu [70] proposed a system that used mammograms as input, which are pre-processed and then analyzed using GLCM to extract features. These features are then used with a decision tree classifier to identify breast abnormalities as either benign or malignant. In diagnosing breast cancer, a decision tree (DT) [71], composed of decision and leaf nodes, is a commonly used classifier because it is easy to define and map the rules from the root to a leaf node thereby resulting in the classification of breast masses into benign and malignant classes. The entropy or in-formation gain computes the homogeneity in the dataset given by:

$$E(S) = -\sum_{x \in X} P(i) \log P(i) \tag{2}$$

The dataset is represented by S, X represents class cardinality and ith class probability is P(i). Zero entropy means perfect classification.

- Naïve Bayes (NB) Classifier: Krishnaveni1 et al. [72] proposed method for analyzing mammogram images extracting the region of interest using chain code, followed by pre-processing through enhancement, then extracting features using Histogram of Oriented Gradients, and finally classifying the image as Benign or Malignant using a Naive Bayes classifier to detect microcalcification. The NB categorizes the data statistically by considering all features. Given the feature set $X = x_1 + x_2 + x_3$, NB computes the posterior probability (probability to be assigned to the unknown instance) of class c, about the type of breast tissues as either benign or malignant, as given by: $P(c|x) = P(x_1|c) \times P(x_2|c) \times P(x_n|c) \times P(c)$. The probability density function of class c is represented by $P(x_i|c)$, whereas the class prior is given by P(c). NB performs well for large datasets, and sometimes, due to the feature set, it outperforms other classifiers [73]. The problem with NB is zero frequency, which occurs when the class and feature combination frequency becomes zero.

- Support Vector Machine Azar and El-Said [74] evaluated the performance of six SVM types in diagnosing breast cancer using the Wisconsin breast cancer dataset, and found that SVM classifiers provided a fast, simple, and efficient method for breast cancer diagnosis. The SVM algorithm finds the optimal hyperplane to separate the classes, allowing for accurate prediction of new, unseen examples. Features such as tumor size, shape, and texture can be extracted and used as inputs to the SVM model, enabling effective breast cancer diagnosis and classification [75]. SVM is a linear classifier that constructs a linear hyper-plane of N-dimensional space to categorize the linear data by maximizing the margin between two classes. Non-linear mapping functions can be used to link the data (source) to a higher dimensional

feature space (target) if the data is non-linear. Training data is used to compute the weighted vector $w = [w_1 + w_2 + w_3 + \ldots.]^T$ and the bias b for discrimination boundary is given by

$$d(X, w, b) = \sum_{i=1}^{n} (w_i x_i + b) \tag{3}$$

where d(X,w,b) is the decision function that is optimal whend(X,w,b)=0. For non-linear data, it is mapped to a high dimensional space using a non-linear linking function as given by

$$K(x_i, x_j) = \phi(x_i)^T \phi(x_j) \tag{4}$$

where $K(x_i, x_j)$ is the kernel function that maps the non-linear mapping function $\phi(x)$. Different studies suggested changing the dataset and adding more constraints (hard margin), the SVM produced good results on mammographic images.

3) DEEP LEARNING APPROACHES

DL is a sub-domain of ML and is the basis of many of the approaches recently reported by many investigators. The basic idea relates to the boosted hidden layers used in shallow neural networks by many of the other time-to-time solutions exploited for the early diagnosis of breast mass abnormality. The schematic diagram of a popular deep learning approach employed for mammography has been illustrated in a step by step manner in Figure 4. DL has an edge over ML due to its self-feature extraction capability (representation learning), significantly improving breast cancer diagnosis [76]. A deep neural network (DNN) is constituted of ''n'' layers and ''m'' hidden neurons. Weights are associated with each input and output link in the neural network. Regulating weights in training helps neural networks learn significant information. The information flows in the learning phase to make it a self-learning network [77]. We have discussed numerous DL-based methods for breast cancer classification and segmentation that use the variants of CNN belonging to one of the three categories (Figure 1): (a) Novel CNNs express impressive results in mammography detection and classification, (b) Transfer Learning (TL) consists of developing a model to use the preset parameters, with salient variants to make the training compatible after adjusting the input size equal to the size of the mammogram with several neurons in the concluding layer set equal to the class-cardinality of the target database, (c) DL feature extraction solutions are based on dynamic feature extraction using the DL models and employed further by conventional ML algorithms to carry out classification tasks. The TL models can also be used for deep feature extraction using customized datasets. An overview of salient DL methods by different authors is given by:

- Bayesian Neural Network: In DL, the Bayesian neural network (BNN) extracts the uncertainties using the Bayesian model, and it refers to the uncertainty of the model output [78]. Specht [79] proposed a Probabilistic
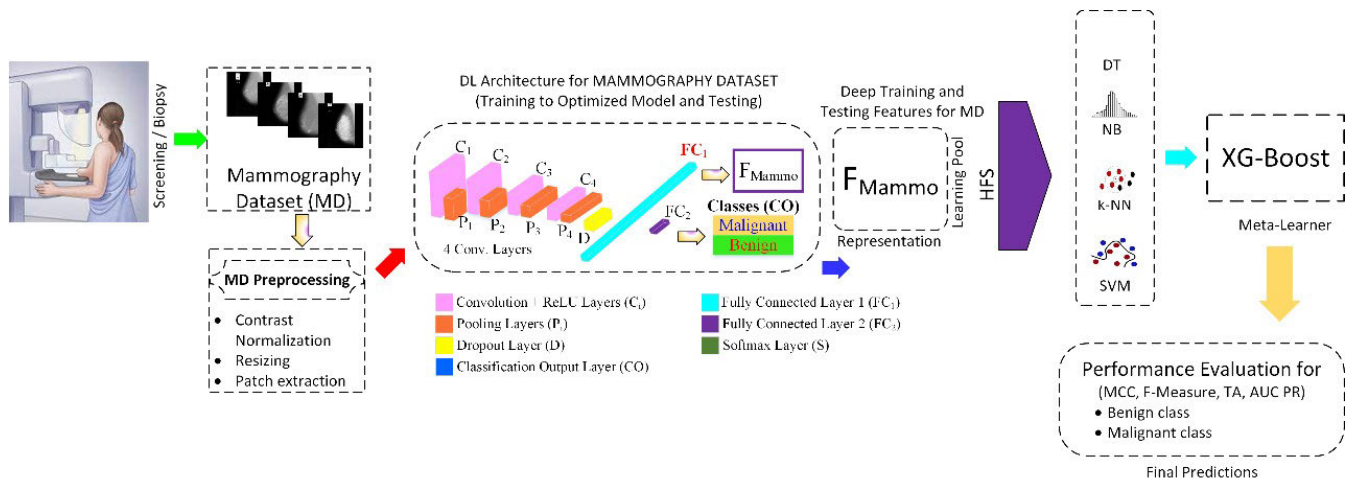
FIGURE 4. Illustration of a prominent DL framework for mammography dataset analysis, where preprocessing techniques such as patch extraction, contrast normalization, and quality control measures are first applied to the dataset. Next, a DL architecture is utilized to extract high-level features from the preprocessed data. A meta-learner is then trained and tested using the output of strong ML classifiers to predict labels and evaluate performance, with metrics such as accuracy, precision, recall, F1-score, and ROC-AUC calculated to assess the model's effectiveness in label prediction.

Neural Network (PNN) based on the Bayesian classification. PNN classified the mammograms into normal, benign, and malignant classes based on the input vector. The feature vector was extracted from a mammogram through Discrete Wavelet Transform (DWT) and then applied classification. Seventy-five (75) images were selected for the experimental purpose, and the accuracy achieved by the authors was 90%.

- Back Propagation in DL: A back propagation neural network (BPNN) is a supervised learning network called a feed-forward neural network with backward propagation of error to adjust the neurons' weights. This neural network consists of an input layer, one or two hidden layers (no hard rule for layers' selection), and, in the end, an output layer. In the BPNN, during the training phase, the features are fed to the neurons for learning. Then, the algorithm fine-tunes the weights based on the error rate (i.e., loss function) from the previous epochs to converge quickly in the backward direction. Zhang et al. [80] proposed a neural network that reduced the false positive rate of microcalcification detection in real cases of 100 patients' mammograms. It consists of a three-stage method. In the first stage, all the microcalcifications were detected. In the second stage, FP detection was removed from the first stage's output. In the third stage, the BPNN with Kalman filter was used for the classification of microcalcification in mammograms.

- Convolutional Neural Network: CNN is a sub-category of deep neural networks that achieves impressive results in mammography for detecting and classifying microcalcifications and is currently the most popular neural network [81]. The classification decision is taken in the decision layer by computing the prediction error or loss function. The first CNN was developed by Fu-kushima et al., known as "Recognition," and was the

very first neural network model used for medical image analysis [82]. The class with minimum loss is declared the classifier decision. Sahiner et al. [83] proposed a backpropagation CNN to classify mammograms. Sub-regions, regions-of-interest (ROIs), are extracted for CNN input. ROI patches are extracted by either averaging, subsampling, or texture feature extraction methods. Lo et al. [84] introduced the Multiple Circular Path Convolutional Neural Network (MCP-CNN), which initially gathered information from the identified regions in mammograms and subsequently processed the features using CNN. Fonseca et al. [85] used an SVM-CNN classifier for breast cancer categorization. Su et al. [86] suggested a method for classifying the breast cancer named "Fast Scanning CNN," where the algorithm computed the pixel-wise image segmentation to remove the redundant information (which increased the original CNN complexity). Jiao et al. [87] presented a method that utilized deep features for breast mass classification. The method combined the intensity-based features with deep features extracted by CNN from the original image and was finally used for classification. Arevalo et al. [88] devised a hybrid approach where they employed CNNs to learn from supervised data representations rather than extracting feature maps directly from mammographic images. Rezaeilouyeh et al. [89] presented a CNN-based model for classification of the breast cancer. In this model, shearlet transform (ST) was applied to the images to get the feature vector of shearlet coefficients fed to classification network. Jadoon et al. [90] developed two DL models using CNN-Discrete Wavelet and CNN-Curvelet transforms for normal, malignant, and benign classes. The extracted features were fed to the classification model. Jaffar [91] introduced a method in which the mammograms are first enhanced; then, the CNN is used for feature extraction,

followed by SVM-based classification. The outcome of their experimentation is discussed in the forthcoming section.

- Regions with CNN (R-CNN): Zhu et al. [92] used a conditional random field and a fully convolutional network model to segment the masses in mammograms. By leveraging prior positional information, the method empirically estimates the ROIs, enhancing the accuracy of ROI predictions. Wang et al. [93] introduced a hybrid method for classifying benign and malignant breast cancer, which involves cropping breast masses and extracting clinical features from multi-view patches of mammograms. CNN was employed to concentrate on regions associated with semantic-based lesions. Gastounioti et al. [94] explained an ensemble method for breast cancer classification. They used lattice-based techniques for textural feature maps and fed them to CNN for multi-class categorization.

  R-CNN is a CNN-based network that detects and classifies data on a regional basis regardless of the class. For this reason, it is also referred to as a Region Proposal Network (RPN). R-CNN reduced the convolution time by selecting a region, which is considered an advantage of using R-CNN. Ribli et al. [15] explained a Faster R-CNN method used for classifying the breast cancer. The feature extraction using Faster R-CNN was based on ROI pooling technique. This method produced bounding boxes accompanied by a confidence score classifying the benign or malignant cancers. Chiao et al. [95] proposed an advanced variant of RPN called Mask R-CNN, which is used to detect and segment mammographic images. Instead of extracting features from the ROI pooling method, the Mask R-CNN employed ROI alignment (ROI-Align) procedure. ROI-Align feature extraction tackled the spatial information loss encountered in Faster R-CNN. Lastly, CNN was used for detection and classification tasks.

- Long Short-Term Memory (LSTM) Neural Network: LSTM is a Recurrent Neural Network (RNN) type that can learn from the reference point instead of from scratch (i.e., error feedback to the input). The reference point is any middle layer whose output can be used as input. As in CNN, the learning must be started from scratch. Gradient vanishing is the major problem in RNN, which is overcome by LSTM, as proposed by Hochreiter et al. [96]. Nahid et al. [97] used LSTM to classify microcalcifications and the formation of masses. They transformed images into 1-D vector format and then converted them into time-series data, followed by LSTM training. The maximum accuracy of 84.4% was achieved when using Softmax at the decision layer.

III. RESULTS
Breast cancer detection has been a conventional problem in medical science since the 16th century. It is still considered the deadliest disease due to its complex morphological

structure. In the early years, breast cancer diagnosis included a self-examination method, which produced many false results. With the advent of mammograms, cancer detection based on imaging became feasible. However, microcalcification or abnormal tissues are very subtle and unstable, making it hard for experienced professionals to detect cancerous tissues early. In recent years, IP techniques have been replaced by computer-aided techniques that help radiologists and experts make more reliable decisions; intelligent algorithms further add classification (to classify cancerous types: benign or malignant), and these techniques produce state-of-the-art, accurate, and more reliable results.

A. DATASETS FOR MAMMOGRAPHY
Mammography datasets play a vital role in designing and developing AI-based solutions, thereby attributing confidence in the scope of the results along with the robustness of the model. Table 2 illustrates large datasets used for conventional machine and DL techniques, along with the corresponding references, total instances, and categories used for classification. The Mammographic Image Analysis Society (MIAS) dataset is one of the pioneering datasets in mammography. It contains 322 mammographic images (digitized at 50 microns pixel edge) [98]. These images are labeled as benign, malignant, and normal. The MIAS dataset has been extensively utilized for developing and validating CAD systems and algorithms to classify breast lesions. It is a widely cited benchmark data set using mammographic images for breast cancer detection research. Similarly, a popular MIAS method is the Mini-MIAS data set [99] (*http : //peipa.essex.ac.uk/info/mias.html*). The Mini-MIAS is a well-known case study in breast screening. It contains 322 mammograms reduced to 200 μm pixel edges and cropped/padded so that each image is 1024×1024 pixels. These mammograms are listed as safe and sensitive, making them valuable for training and experimental computer-aided detection programs. The dataset has been widely used to develop and evaluate algorithms for breast cancer detection and classification, which is a benchmark in medical image analysis.

DDSM (Digital Database for Screening Mammography) is a comprehensive database specially developed for research in mammographic image analysis. It contains a collection of 2620 scanned film mammography examinations labeled normal, benign, and malignant, as well as associated clinical data and ground truth descriptions [100] (http://www.eng.usf.edu/cvprg/Mammography/Database.html). It is a valuable resource for developing advanced IP techniques such as detection and classification algorithms for breast cancer detection Due to its size, diversity, and fine resolution, the DDSM dataset is widely used in academia and engineering in a research environment. The Curated Breast Imaging Subset of the DDSM (CBIS-DDSM), a standard for performance and accuracy, is a curated dataset designed for breast cancer detection and diagnostic screening. The CBIS-DDSM

data set consisted of 10239 standard mammograms to facilitate the creation and evaluation of computer screening algorithms, and other image analysis techniques developed for mammography [101] (https://wiki.cancer image database.net/display/Public/CBIS-DDSM). Due to its comprehensive description, image quality, and focus on analysis and diagnostic information, the CBIS-DDSM dataset has become a widely used benchmark in mammographic image analysis. The IRMA (Image Retrieval in Medical Applications) dataset from RWTH Aachen University in Germany serves as a collection of mammogram patches designed to assess the accuracy of mammogram patch classification methods [102]. It includes datasets from MIAS, DDSM, Lawrence Livermore National Laboratory (LLNL), and regular images from RWTH Aachen. The dataset provides detailed information about the images, classifying them based on background nodes and the nature of abnormalities detected in the mammogram patch. The mammogram patches in the dataset are standardized as 128×128 pixels, with 931 normal, and 584 abnormal images.

The BancoWeb LAPIMO dataset is a mammographic image dataset specially developed for research purposes in breast cancer detection [103] (http://lapimo.sel.eesc.usp.br/bancoweb). Based on 1400 images from 320 patients, this dataset is designed to support the development of ML/ DL algorithms and other image analysis techniques tailored for mammography. The digitized mammograms are normal, benign, and malignant, with detailed annotations and ground truth labels indicating the presence of various types of lesions, such as masses and calcifications. The INBreast is a mammographic image dataset designed to support research in breast cancer detection and diagnosis [104]. It was created by the Faculty of Medicine of the University of Porto, Portugal, and consists of a collection of 410 mammograms obtained from both screening and diagnostic examinations (https://www.kaggle.com/datasets/ramanathansp20/inbreast-dataset). This dataset includes images with numerous breast abnormalities, such as masses, calcifications, and asymmetries, along with detailed annotations and ground truth labels provided by expert radiologists. Over and above, the King Abdulaziz University Breast Cancer Mam-mographic Dataset (KAU-BCMD) [105] (https://www.kaggle.com/datasets/asmaasaad/king-abdulaziz-university-mammogram-dataset) is a mammo-graphic image dataset designed to support research in breast cancer detection and diagnosis. This dataset consists of a collection of digital mammograms accompanied by detailed annotations and ground truth labels provided by three radiologists. The ordinal categorization of cancer is based on the breast imaging reporting and data (BI-RAD) classification system. The VinDr-Mammo, a Vietnamese dataset of digital mammography developed by VinBigData, is a research initiative by Vingroup JSC aiming to advance healthcare through ML [106] ($https://doi.org/10.13026/br2v-7517$). This dataset comprises an extensive collection of digital mammograms, categorized on the ordinal states of the BI-RAD classification system

for extensive lesion-level annotations and dam-age-level assessment, with detailed annotations and ground truth labels provided by the three expert radiologists. The acronyms for some recent DL techniques are illustrated in Table 3 with the dataset used and the method adopted.

1) IMAGE PROCESSING

The subsection describes some IP-based studies used for breast cancer analysis by mammography. In this study, salient image-based techniques are briefly reviewed in the initial part, where prominent algorithms are surveyed. In this context, Verbeek et al. [35] analyzed data according to the age groups of women, where the odds ratio of 0.48 (confidence interval $= 95\%$) was used. Further, the study was conducted for unscreened objects as well. The fatality rates of both, screened/unscreened subjects, were then compared based on breast cancer. Rangayyan et al. [40] employed the Adaptive Neighborhood Contrast Enhancement (ANCE) method, represented the digitization down-sampling to an adequate pixel size and consequently degraded images affecting the radiologist's decision. The use of the ANCE technique assisted the radiologist's performance. The area parameter of an ''enhanced mammogram'' was found to be 0.6745 which was higher than the digitized and original mammograms. In another study, Carney et al. [37] correlated Hormone Replacement Therapy (HRT) with age and microcalcification density, and its role in screening accuracy performance. By adjusting breast density ranges between $(62.9-87.0)\%$ from highly dense to fatty breasts, they found that the sensitivity increased from 68.6% to 83.3% with age. Matsubara et al. [108] used an adaptive thresholding scheme dividing the mammogram so that the tissues in it are divided into one of the three classes based on histogram analysis ranging from fatty to dense classes. The affected regions containing potential masses are detected by using multiple threshold values. Dominguez and Nandi [109] based segmentation on the conversion of mammograms to binary images at selected threshold levels. They used 30 gray levels with a minimum step of 0.025 with 8-bit gray levels between 0 and 1. The segmentation sensitivity was 80% with the proposed method. Zheng et al. [114] introduced a region growth mechanism for initial boundary conditions of adaptive contouring of the mass region in the mammogram. The final contour of mass was achieved by using a contour algorithm working runtime dynamically. For 85 queried regions, in an observer preference study, a scheme was based on referenced regions divided into two sets, and the previously randomly selected regions were compared with the queried sets. In 54.1% of the examined regions, the four observers chose the reference image set that was visually more similar when compared to the queried region. Zou et al. [115] proposed a deformable model for parametric contouring using partial differential equations for the determination of gradient vector flow field, yielding an accuracy of 82.6%. After the enhancement of mammographic images with adaptive histogram equalization,

TABLE 2. Large publicly shared datasets in the field of mammography (B: benign, M: malignant, N: normal, (x) indicates the severity of disease according to the BIRAD classification system).

Dataset	Number of Images	Classes	Year
MIAS (50 microns) [98]	322	B, M, N	1994
Mini-MIAS (200 microns) [99]	322	B, M	1994
DDSM [100]	10480	B, M, N	1999
CBIS-DDSM [101]	10239	B, M, N	2017
IRMA [102]	1515	B, M, N	2009
BancoWeb LAPIMO [103]	1400	B, M, N	2011
INBreast [104]	410	B, M, N	2010
KAU-BCMD [105]	5662	B(2), M(5), N(1)	2021
VinDr-Mammo [107]	5000	B(2), M(5), N(1)	2022

TABLE 3. Acronyms and their full description, datasets, and methodology in determining microcalcification for some state-of-the-art techniques.

Microcalcification Method	Acronym	Dataset	Method	Authors	Ref.
Mean Multi-Scale 2D NEO, Max Multi-Scale 2D NEO	MnM2DNEO, MxM2DNEO	DDSM, INBreast, PGIMER-IITKGP	Data reduction approach based on data distribution	Karale et al.	[110]
Anomaly Separation Network	ASN	INBreast	Hybrid approach (generative plus discriminative)	Zhang et al.	[111]
Max Multi-Scale 2D NEO, Mean Multi-Scale 2D-NEO	Modified MxM2DNEO, Modified MnM2DNEO	DDSM, INBreast, PGIMER-IITKGP	Computer-aided diagnosis	Karale et al.	[112]
Unsharp masking	Unsharp masking	DDSM, private database	Contrast enhancement between microcalcifications and background	Karale et al.	[113]

the GVF field component with the larger entropy was used to generate the ROI. Yuan et al. [116] employed a Full-Field Digital Mammography (FFDM) image to highlight abnormal masses from the surroundings using a dual-stage procedure. Firstly, the initial contour is determined using index-based segmentation using radial gradients. Secondly, a contour model is used dynamically for the region segmentation to find the abnormal mass contour. The distance feature outperformed using the leave one out method using lesion-size, and contrast, and distance features, yielding the AUC (ROC) = 0.86. Similarly, Hassanien and Ali [117] proposed an algorithm for segmenting abnormal masses using fuzzy sets with Pulse Coupled Neural Networks (PCNN). Before segmentation, the fuzzy histogram hyperbolization is applied as a filter, followed by PCNN. Although, the IP methods are very old, they are being used as preprocessing support to exploit the feature space for AI-techniques.

B. MACHINE LEARNING

This section surveys the ML-based approaches for the detection and classification of breast cancer. In this context, numerous methods have been accumulated spanning over time, emerging for mammography datasets focusing on different aspects of the problem domain. Davies and Dance [56] studied three-step mammogram en-hancement before classification. A TP of more than 85% was reported with an image count of 78 during the testing phase. The Frame Texture Classification Method (FTCM) was used for the classification of abnormalities in mammograms. Local thresholding was used, where the calcification was segmented from the background for further classification of images. These studies reported the true positives (TP) of 100% by testing the methodology on 50 images. Rad et al. [55]

used a multi-wavelet-based feature extraction technique and features used for training the classifiers and achieved an accuracy of 85%.

Caldwell et al. [118] computed the correlation between the fractal dimensions to mammograms by experimenting with NB and SVM classifiers. The study reported an accuracy of 84% (radiologist-approved) using 70 mammographic images. Zheng et al. [119] used a Bayesian network in which an acyclic graph is used to compute probability influences between features. By experimenting with a dataset of 433 images and 12 features, the authors reported AUC (ROC) curve equal to 0.87. The Nijmegen database was used in this study to test the methodology on 40 images. In another study, 180 images from the Nijmegen LLNL/UCSF database were tested by the k-NN classifier. It was trained on three categories of extracted features (a combination of statistical and multi-resolution) and reported an accuracy of 80% [120]. Cao et al. [121] investigated the additional benefit of peri-calcification areas in contrast-enhanced mammography for distinguishing between breast lesions appearing solely as calcifications on standard mammograms. They analyzed radiomic characteristics from both low-energy and recombined images within the calcification sites and their surrounding peri-calcification regions. These regions were defined by extending the an-notation margin radially with gradients ranging from 1 mm to 9 mm. ML models were employed to categorize cal-cifications as either malignant or benign. In another effort, Prinzi et al. [122] presented a radiomic signature aimed at effectively distinguishing between healthy tissue, benign microcalcifications, and malignant micro-calcifications. Radiomic features were extracted from a proprietary dataset that included 380 samples of healthy tissue, 136 samples of benign microcalcifications, and 242 ROIs with malignant microcalcifications. Following this, two

separate signatures were identified for detecting healthy tissue versus microcalcifications and for the classification of benign versus malignant microcalcifications. Various ML models, including SVM, RF, and XGBoost, were used as classifiers. The performance of the models was assessed, with XGBoost achieving an AUC (ROC) of 0.830 for healthy tissue classification, 0.856 for benign microcalcifications, and 0.876 for malignant microcalcifications. Yoen et al. [123] investigated factors linked to abnormality scores generated by AI software. They performed a retrospective search in a database to identify a series of asymptomatic women who had undergone breast surgery from 2016–2019. Preoperative mammograms were evaluated using AI software (LunitINSIGHT) to assign abnormality scores. A score greater than 10 indicated positive detection of an abnormal lesion. A general linear model was employed to analyze the mammographic and pathological findings along with clinical repercussions associated with the AI software scores. Similarly, Malek et al. [124] introduced a method for filtering and extracting features utilizing persistent homology (PH), a robust mathematical tool for analyzing intricate datasets and patterns. Instead of directly operating on the image matrix, the filtering process is conducted on the diagrams derived from PH, enabling the identification of significant image characteristics amidst noise. They used the DDSM and MIAS datasets for their experiments with supervised ML-models. The study demonstrated that selecting a suitable PH filtering with dis-criminative features can increase the performance score of early cancer detection.

Khalid et al. [125] introduced an effective DL model to detect breast cancer in computerized mammograms of varying densities. Their approach involved feature selection by elimination of high-bias and repeating features. The model was evaluated using 3002 merged images who underwent digital mammography between 2007 and 2015. Additionally, six classification models were applied for breast cancer diagnosis, including RF, DT, k-NN, LR, and SVM. The study demonstrates that the proposed model achieved high efficiency, requiring minimal computational resources while maintaining a high accuracy score. Li et al. [126] used adaptive and multi-scale processing techniques to create a novel CAD mass detection system that improved sensitivity, specificity, and robustness against fluctuations in mammography. Using the dataset, they integrated hard and soft categorization through a modified fuzzy decision tree and committee decision-making method. This approach enabled them to achieve an AUC (ROC) of over 0.9. Iseri et al. [127] developed a novel method for the classification of microcalcification clusters employing a mul-ti-window-based statistical analysis (MWBSA) method. This method uses a two-stage software framework as a computational search and analysis system, with an artificial neural network (ANN) as a classifier. Experimental results on different datasets with MIAS and DDSM are also presented. Datasets showed that the MWBSA-based strategy was as successful

as other well-known methods such as GLCM and Wavelet techniques. Their classification task achieved a 97% accuracy rate. Rampun et al. [128] presented a novel investigation of ML performance by examining prob-ability outputs in con-junction with classification accuracy score and AUC for ROC curve. They used the CBIS-DDSM database1872 micro-calcification clusters. They experimented on Random Forest (RF), Multi-layer Perceptron (MLP), Logistic Regression (LR), Naive Bayes (NB), Bayesian Network (BNet), k-NN, Alternate Decision Tree (AD-Tree), Logistic Model Trees (LMT), AdaBoostM1(AdaBoost) and SVM.

Further, Fanizzi et al. [129] suggested a binary classification model for differentiating tissues in digital mam-mograms to support radiologists in their work. They specifically examined the impact of various techniques on the feature selection procedure concerning the chosen features and learning performances. They extracted textural features using Haar wavelet decompositions for each ROI, as well as interest spots and corners that were found using the Minimum Eigenvalue Algorithm (MinEigenAlg) and Speeded Up Robust Feature (SURF). Next, a subset of features was chosen using two distinct feature selection methods, namely filter and embedding methods, used to train an RF binary classifier. For the benign/malignant and normal/abnormal situations, the prediction performance achieved the accuracy and median AUC (ROC) values as (97.31% and 0.88), and (98.16% and 0.92), respectively. Vy et al. [130] created a machine-learning classification model that would use clinical factors, mammography results, ultra-sound results, and histopathological features to distinguish between ductal carcinoma in situ (DCIS) and minimally invasive breast cancer (MIBC). Using a trained XGBoost algorithm, tumors were classified as DCIS or MIBC using the five most significant clinical characteristics including calcification on mammograms. XGBoost model attained AUC (ROC) and accuracy of 0.93 and 84%, respectively, comparable to that of a skilled radiologist in distinguishing be-tween DCIS and MIBC and providing patients with the most excellent possible therapy options. Sarvestani et al. [131] assessed the practicability and precision of automatically separating images of micro-calcifications in the breast tissue. The decision tree classification approach was used to classify the breast tissue microcalcification clusters that have been identified. ANN was employed to identify the benign and malignant forms of segmented ROI clusters. The DDSM was used to train the proposed system. After training, the model led to an improved generalization of 93%. Lin et al. [132] showed that an automated deep-learning pipeline can facilitate early breast cancer diagnosis for mammography microcalcifications detection and classification. The system's development and testing utilized a total of 4,810 images from various centers. For both the training and test sets, the overall classification accuracy values for differentiating benign and malignant breasts were 72.37% and 81.24%, respectively. Their automated artificial intelligence system was claimed to

have the potential to enhance the decision-making abilities of clinicians by helping them identify, diagnose, and treat breast cancer more effectively. Fu et al. [133] proposed a two-step detection model. First, the location and nature of potential microcalcifications were determined using a mathematical model. It was investigated that the proposed model could accurately detect micro-calcification events when tested in the Nijmegen University Hospital database. Second, after extracting the features of each putative microcalcification, the sequential forward search (SFS) method was applied to identify sensitive attributes for microcalcifications. The classification performance of SVM and general regression neural network (GRNN) in terms of AUC (ROC) were 0.98 and 0.97, respectively, using the test data set.

Computer-assisted breast cancer detection from mammograms was introduced by Golobardes et al. [134]. Firstly, several microcalcification feature extraction techniques were used on the mammograms. Secondly, automatic diagnosis was obtained by applying several ML algorithms. The authors examined the use of these characteristics as a classification system to differentiate between benign and malignant microcalcifications in mammograms taken from the mammography database of the Girona Health Area. They achieved a maximum accuracy of 78.57%. Similarly, Alolfe et al. proposed a four-step approach to developing intelligent diagnostic systems [135]. These steps were (a) the selection of ROIs, (b) the use of wavelet decomposition as the basis for the feature extraction step, (c) the selection of features, and (d) the classification of the results. The SVM classifier and the voting k-NN classifier were utilized in the classification stage. The MIAS mammographic datasets comprising 322 mammograms were used to assess the suggested method. SVM yielded the best accuracy of 87.5% of the potential classifiers tried, whereas k-NN produced the best accuracy of 75%. Using the Nijmegen and MIAS mammographic databases, Papadopoulos et al. [136] demonstrated a novel automated system for characterizing microcalcification clusters in three phases (cluster detection, feature extraction, and classification). A rule-based system, an ANN, and an SVM were constructed and assessed during the classification stage using the ROC analysis. A comprehensive comparison of evaluations of some ML-based techniques is illustrated in Table 4.

In this review article, we have consolidated key performance metrics (AUC, sensitivity, specificity) from some articles, providing a clear picture of model performance. Summarizing these metrics allows us to concisely convey essential insights without including exhaustive confusion matrices, as illustrated in Table 5.

C. DEEP LEARNING

Convolution Neural Network (CNN) is mainly used for DL. A CNN is constituted of n layers and m hidden neurons. Weights are associated with each input and output link in the neural network. Regulating weights in training helps

neural networks to learn significant information, known as representation learning. The information flows in the learning phase to make it a self-learning network. CNN achieves impressive results in mammography for classifying the microcalcifications. Depending on the complexity of mammograms, features are hidden locally in mammograms that exhibit similar information, so it is tough to recognize abnormalities. The changes made in the CNN architectures were mainly in the input size, depth and size of kernels, activation functions, surviving fractions of neurons in the drop-out layer, fully connected layers' specifications, and the decision layer.

In a study by Sahiner et al. [83], regions of interest are extracted for CNN's input. The back-propagation technique is used to train the CNN. The area under the curve was 0.87, while 90% and 30% of TP and FP were reported in this study. The results were computed on the test dataset comprising 168 images. Moreover, MCP-CNN is classified based on mass features extracted from mammograms [84]. The area under the ROC curve of 0.89 was reported when taking 144 mammograms to evaluate the proposed model. Fonseca et al. [85] presented CNN-SVM model for the breast cancer classification and reported a Kappa value of 0.58. Wu et al. [137] employed the convolution neural network for the classification of microcalcifications into benign and malignant categories. The pixel values of mammograms are considered global features and fed to CNN. After testing the methodology using 40 images, the sensitivity and specificity score was 75% for each. Furthermore, TL and CNN were used for the classification of the breast cancer dataset by Huynh et al. [138]. For ensemble and analytical extracted features, the AUC (ROC) was 0.86 and 0.81 respectively. The study used 219 mammograms for the evaluation of the methodology. Jiao et al. [87] combined intensity featurtes and deep features for classification of the original images. The accuracy of 96.7% and 97.0% were achieved for CNN and VGG-based models using the DDSM dataset for the training and testing process. A hybrid approach was proposed by Arevalo et al. [88] to classify mammograms. Upon using 736 mammographic images, the area under the ROC curve of 0.89 was achieved. Jadoon et al. [90] used the IRMA dataset for their experimentation. For testing, 2796 ROI patches from mammograms were used and achieved accuracy scores of 81.83% and 83.74% from CNN-DW and CNN-CT respectively. Another study used CNN to focus on semantic regions and the Recurrent Neural Network (RNN) was used to classify breast cancer. The study was performed by Wang et al. [93] and reported an accuracy of 89% using 763 images from the Breast Cancer Digital Repository. Gastounioti et al. [94] used Lattice-based techniques to extract texture feature maps and fed them to the multichannel CNN. Upon using 106 cases for evaluation, an accuracy score of 90% was reported.

Jaffar [91] used CNN for feature extraction and an SVM was applied for the classification of Mini-MIAS and DDSM datasets. An accuracy of 93.35% and sensitivity of

TABLE 4. A comparison of the evaluation of ML models for classification tasks using mammograms.

Reference	Data	ML Model/Algorithm	AUC (ROC)	Accuracy (%)
[56]	A dataset of 75 images, 25 training and 50 test images	Nearest neighbor clustering algorithm with nearest neighbor distance less than 5mm between calcifications	×	92.00
[65]	The dataset of 40 images	Multi-wavelet-based feature extraction technique	×	85.00
[118]	Experiments based on 70 images	Fractal-based Wolfe grade classifier	×	84.51
[119]	The dataset of 433 images	Bayesian belief network (BBN)	0.87	80.00
[120]	The data consisted of 180 images	k-NN classifier	×	80.00
[121]	The mammogram test set included patients between March 2017 and March 2019, while the validation set was collected between April 2019 and October 2019	Ensemble classifier	0.89	84.30
[122]	Comprising 380 samples of healthy tissue, 136 samples of benign microcalcifications, and 242 samples of malignant microcalcifications	SVM, RF, and XGBoost	0.83, 0.85, 0.87 for healthy, benign, and malignant microcalcification, respectively	74.00, 81.10, 82.40 for healthy, benign, and malignant microcalcification, respectively
[123]	A database with consecutive asymptomatic women who underwent breast cancer surgery between (2016-2019)	LunitINSIGHT, MMG, Ver. 1.1.4.0 as a diagnostic tool	×	72.00
[124]	MIAS and DDSM public mammography datasets	Neural network (NN), SVM, k-NN, and DT models	0.95 - 0.98	94.30 - 96.40
[125]	3002 merged images from 1501 individuals (between Feb-2007 and May-2015)	RF, DT, k-NN, logistic regression (LR), linear SVM	×	96.49
[126]	Training: 30 normal and 47 abnormal images Testing: 100 normal and 39 abnormal images	Modified fuzzy decision tree	> 0.90	×
[127]	119 images from MIAS and DDSM databases	Multi-window based statistical analysis (MWBSA) for detection of microcalcification clusters, and ANN	×	97.00
[128]	1872 micro-calcification clusters (1199 benign and 673 malignant) from 753 patients	C4.5, RF, MLP, LR, NB, BNet, k-NN, ADTree, LMT, AdaBoost, and SVM	0.82 (ADTree)	77.80 (C4.5)
[129]	260 ROIs extracted from BCDR mammograms	RF binary classifier	0.98 (benign), 0.92 (malignant)	97.31 (benign), 88.46 (malignant)
[130]	Mammographic, clinical, and sonographic features from 420 patients	XGBoost	0.93	84.00
[131]	DDSM dataset	ANN	×	93.00
[132]	4810 mammograms with 6663 microcalcification lesions	ResNet50 for feature extraction, and FasterRCNN for microcalcification detection	0.80	72.37
[133]	Nijmegen University Hospital (Netherlands) database	Sequential forward search (SFS) algorithm on General regression neural network (GRNN) and SVM	0.98 (SVM), 0.97 (GRNN)	×
[134]	216 mammograms from the database of Girona Health Area	CBR and GA	×	78.57 (Max)
[135]	322 images of MIAS dataset	Wavelet analysis, feature selection method, k-NN, and SVM	×	87.50 (SVM best), 75.00 (k-NN best)
[136]	MIAS dataset	SNM, and ANN classifiers	0.79 (Nijmegen), 0.81 (MIAS)	×

TABLE 5. A comprehensive look at ML metrics for improved detection and classification of breast cancer.

Category	Metric	Value/Description	Reference
General Metrics	AUC (Detection)	RF: 0.859, SVM: 0.865, XGBoost: 0.854	[122]
	AUC (Classification)	RF: 0.921, SVM: 0.927, XGBoost: 0.933	
	Sensitivity (Detection)	RF: 0.729, SVM: 0.783, XGBoost: 0.702	
	Sensitivity (Classification)	RF: 0.931, SVM: 0.863, XGBoost: 0.909	
	Specificity (Detection)	RF: 0.782, SVM: 0.794, XGBoost: 0.794	
	Specificity (Classification)	RF: 0.781, SVM: 0.875, XGBoost: 0.750	
Before and After CAD	Specificity (%)	Before: 90.2, After: 87.2 (P < 0.001)	[7]
	Sensitivity (%)	Before: 80.4, After: 84.0 (P = 0.32)	
	Positive Predictive Value (PPV)	Before: 4.1, After: 3.2 (P = 0.01)	
	Biopsy Rate	Before: 14.7, After: 17.6 (P < 0.001)	
	Cancer Detection Rate	Before: 4.15, After: 4.20 (P = 0.90)	
	AUC	Before: 0.919, After: 0.871 (P = 0.005)	
Specific Scenarios	Sensitivity (Microcalcifications Only)	SVM: 0.93, k-NN: 0.95	[8]
	Specificity (Microcalcifications Only)	SVM: 0.79, k-NN: 0.74	
	AUC (Microcalcifications Only)	SVM: 0.85, k-NN: 0.84	
	Sensitivity (Breast Masses Only)	SVM: 1.0, k-NN: 1.0	
	Specificity (Breast Masses Only)	SVM: 0.26, k-NN: 0.21	
	AUC (Breast Masses Only)	SVM: 0.60, k-NN: 0.57	
	Sensitivity (Microcalcifications + Masses)	SVM: 0.95, k-NN: 0.94	
	Specificity (Microcalcifications + Masses)	SVM: 0.78, k-NN: 0.76	
	AUC (Microcalcifications + Masses)	SVM: 0.85, k-NN: 0.83	
Confusion Matrix Overview	Irregular	96 (76%) detected	[13]
	Lobular	83 (71%) detected	
	Oval	26 (84%) detected	
	Round	16 (89%) detected	
INbreast Dataset	AUC	0.95 (95% CI: 0.91–0.98)	[15]
	Sensitivity (Lesion Detection)	90%	
	False Positives	0.3 marks per image	
	Specificity (Mammography)	Range: 89%–97%	

93.00% were achieved. In another research by Chakravarthy and Rajaguru [139], the ResNet-18 was used for feature extraction with the proposed improved crow-search optimized extreme learning machine (ICS-ELM). The proposed framework was experimented using DDMS, MIAS, and INbreast datasets. The accuracy scores of 97.193, 98.137, and 98.266% were obtained for DDSM, MIAS, and INbreast datasets respectively. Ueda et al. [140] used VGG-16 on the IDC dataset and reported a 61-70% accuracy score for the classification. The DCNN system with autoencoder-genrative adversarial network (A-GAN) was proposed for mammogram images by Swiderski et al. [141] who leveraged the GAN architecture to augment mammogram data by generating additional image representations, enriching the analysis with more diverse information. The generated images were combined with the original mammograms and used as input for a CNN, serving as the final classifier. This DL system was designed to classify mammograms into two categories: normal and abnormal. The results showed that this approach outperformed existing methods for mammogram recognition, highlighting its potential for improved diagnostic accuracy. The detection rate was reported at 89.71% for breast masses. Xu et al. [142] used a Multi-Scale Attention-Guided Network (MSANet) and achieved an AUC (ROC) as 0.94 when experimenting DDSM dataset. Furthermore, AlexNet, DenseNet, and ShuffleNet were experimented with using the INbreast dataset by Huang et al. [143]. The

accuracies for test partitions using AlexNet, DenseNet, and ShuffleNet were 95.46%, 99.72%, and 97.84%, respectively. Recently, to test the accuracy of two large language models (LLMs), ChatGPT-4 and Gemini, Haider et al. [144] created 50 real-life scenarios related to breast health. They scored their responses from 0 to 2, where 0 meant incorrect, 1 meant partially correct, and 2 meant completely correct. They compared their performance using statistics. Gemini performed better overall, getting 98% of the answers correct, while ChatGPT-4 got 71% correct. Both models did well in two areas, but Gemini did better in three other areas, including classifying breast tissue, breast shape, and breast sagging.

Zebari et al. [145] worked on classification of benign and malignant tumors using mammograms. ROI was derived using hybrid thresholding and ML method. It was then separated into five blocks, and noise removal was carried out by applying wavelet transform. Multiple features were extracted using multifractal dimension approach and then features were reduced using genetic algorithm. They used five classifiers, and the final decision was made by fusing the results of all the blocks. The model was evaluated on four mammography datasets, and an accuracy of greater than 96% was achieved. Recently, Nomani et al. [146] presented a breast cancer detection model using ML based on particle swarm optimized wavelet neural network (PSOWNN). Dimension reduction was carried out through PCA, and each image was manually cropped to obtain ROI. Features were extracted using a

TABLE 6. A comparison of the evaluation of DL architectures for classification tasks using mammograms.

Ref.	Data	DL Architecture	AUC (ROC)	Accuracy (%)
[83]	Manually extracted ROI's from 168 mammograms	CNN (4 conv.) with 2 input images, 3 image-groups in the first hidden layer, 2 groups in the second hidden layer, and one real-valued output	0.87	×
[84]	200 mammograms selected from MIAS database and BAMC database	MCPCNN	0.86 (mean)	×
[85]	Digital images obtained from 1157 subjects (Lima, Peru)	CNN (3 conv.) and SVM classifier	×	73.05 (mean)
[138]	607 mammography images	An ensemble of SVM1 (TL-features using AlexNet), SVM2 (analytically detected features, TL-based classifier, and analytical feature extraction-based method)	0.81	×
[87]	600 images from DDSM	CNN (5 conv., 3 fc)	×	97.00
[88]	736 film images	CNN (2 conv., 1 fc, and a softmax layer)	0.82	×
[90]	IRMA dataset: 2796 patches of mammogram images	CNN-discrete wavelet, and CNN-curvelet transforms	×	81.83 (CNN-DW), 83.74 (CNN-CT)
[91]	MIAS: 332 images, DDSM: 1800 images	CNN(3 conv., 1 fc) with SVM	0.93	93.35
[93]	BCDR-F03: 736 film images	CNN with attention mechanism integrating features by LSTM, and classification by multi-view CNN	0.89	85.00
[94]	424 mammogram images	CNN(2 conv., 1 fc) gives five features that are fed to a logistic regressor	0.90	×
[137]	80 ROIs selected from digitized radiographs	CNN (1 conv.) with one hidden layer using seven kernels	0.83	×
[139]	DDSM, MIAS, and IN-breast datasets with 570, 322, and 179 mammograms, respectively	ResNet-18 with ICS-ELM	×	97.19, 98.14, and 98.27 for DDSM, MIAS, and INbreast datasets, respectively
[140]	IDC dataset (1119 images)	VGG-16	×	61.00-70.00
[141]	11218 regions of interest of mammographic images from the DDSM	A-GAN plus CNN	0.94	89.71
[142]	DDSM dataset with 2620 cases having four mammograms each	Multi-Scale Attention-Guided Network (MSANet)	0.94	×
[143]	INbreast dataset	AlexNet, DenseNet, and ShuffleNet	×	95.46, 99.72, 97.84, respectively
[145]	Mini-MIAS, DDSM, IN-breast, and BCDR contributing: 316, 981, 200, and 736 mammograms, respectively	ANN (Multilayer perceptron)	×	>96.00
[146]	Mini-MIAS: 1824 images	CNN (3 conv., 3 fc)	×	95.20
[147]	DDSM: 2620 images, IN-breast: 410 images, MIAS: 326 images	CNN (3 conv., 2 fc)	0.97 (mean)	97.49 (mean)
[147]	Breast cancer risk factor assessment dataset: 88763 images	CNN (AlexNet, ResNet101, and InceptionV3)	×	91.30 (InceptionV3)
[149]	Mini-DDSM: 9752 mammograms	CNN (AlexNet, VGG16, ResNet50)	0.86 (AlexNet)	65.89 (AlexNet)
[150]	CBIS-DDSM: 6671 images, DDSM: 2620 images	CNN (12 conv., 4 dropout layers)	0.98 (mean)	100 (binary classification), 95.80 (multiclass)
[151]	CBIS-DDSM	CNN (four optimizers)	0.96	94.00
[152]	CBIS-DDSM, and Breast Cancer Wisconsin (BCW) containing 3400 mammographic images	AlexNet, Fuzzy C-Means clustering algorithm, and multiple classifiers	×	98.84

TABLE 6. *(Continued.)* A comparison of the evaluation of DL architectures for classification tasks using mammograms.

[153]	168 full-field digital mammography exams (248 images from 168 patients)	Local features with an unsupervised k-means clustering algorithm and LightGBM classifier	0.73 (clustering)	53.00
[154]	384 patients with 414 pathologically confirmed microcalcifications (221 malignant, 193 benign)	DL model with mammography and clinical variables	0.91	×
[155]	298 mammographic images from 149 patients	CNN (5 residual layers, 0.25 dropout)	0.86	86.70
[156]	ADMANI dataset (28911 instances) by the Radiological Society of North America (RSNA)	CNNs and ViT architectures with data augmentation techniques	0.88	89.00
[157]	Contrast Enhanced Mammography (CEM) images of 1601 patients at Maastricht UMC+, and 283 patients at Gustave Roussy Institute	DL model and handcrafted radiomics-based technique	0.95	×
[158]	1000 patients, 1986 mammograms with 389 malignant, 611 benign groups of microcalcification	AlexNet, ResNet18, and ResNet34	0.88-0.92	×
[159]	348 radiomics images (mammograms) and deep features (X-ray) from the Eindhoven Cancer Dataset	CNN with Transformer	0.91	92.00
[160]	200 cases of mammograms from the BI-RADS II	R-CNN model with DL radiomic features	0.89	87.50
[161]	MIAS dataset	KNN algorithm	0.96	×
[162]	1181 mammogram images	CNN and transfer learning with DenseNet201, MobileNetV2, and EfficientNetB7	0.92	×
[163]	211 mammograms from private dataset	InceptionV3 model and multiclass classifiers (SVM, kNN)	0.94	96.80 (SVM)
[164]	3148 images, from DDSM	RetinaNet, and VGG19	0.92	×

gray-level co-occurrence matrix. The model was verified using a published dataset, and it correctly classified 95.2% of the 905 images. Maqsood et al. [147] worked on a DL breast cancer detection system for early diagnosis using an end-to-end training strategy. Initially, a contrast enhancement method was used to refine the edges of mammogram images. The classification performance was enhanced using transferable texture CNN (TTCNN) and energy layer employed to extract texture features. The model consisted of three layers of convolution and one energy layer. Deep features were extracted and feature selection was carried out using firefly method (entropy controlled). Three public datasets were used, and an average accuracy of 97.49% was achieved.

Further, Lin et al. [148] developed a DL model for breast cancer diagnosis. Data classification was carried out using ANN and SVM. TL-based DL architectures (ResNet101, AlexNet, and InceptionV3) were analyzed using advanced statistical techniques, like adaptive moment estimation with stochastic gradient descent. The model was verified using a breast cancer risk factor dataset, and an average accuracy of 94.2% was obtained. Mohapatra et al. [149] evaluated the performance of various CNN architectures by training

through weights reset (from scratch) and others through TL (pretrained). A small public mammography dataset was used for this study, and data augmentation by rotation and zooming techniques was applied to overcome overfitting. AlexNet and VGG16 showed an accuracy of 65%, while ResNet50 showed an accuracy of 61%. Al-Tam et al. [150] developed a hybrid DL framework for breast lesion detection. The backbone residual DL network was utilized for feature extraction, while the transformer was used for breast cancer classification. Two publicly available datasets were used to verify the model, and an accuracy of 100% for binary and 95.8% for multiclass categorization was achieved using 5-fold cross-validation. In their work, Kumar et al. [151] employed CNNs with four distinct optimizers, utilizing input images sized at 299 × 299 × 3. Feature mapping was achieved through a pretrained InceptionResNetV2 model. Evaluation of a curated subset of the DDSM mammogram dataset showcased superior performance in sensitivity, specificity, accuracy, and AUC (ROC) compared to previous DL and classical ML approaches.

Another study introduced a fully automated system for diagnosing breast cancer, utilizing an AlexNet and multiple classifiers to attain heightened accuracy level. Validation

through testing on three Kaggle datasets confirmed its superior performance, indicating its potential utility in aiding medical professionals with precise diagnosis [152]. Marathe et al. [153] introduced a quantitative method to differentiate between benign and actionable amorphous calcifications on mammograms. This method utilizes local textures, global spatial relationships, and expert features. The approach, trained and validated on 168 digital mammography exams, demonstrated high sensitivity and positive predictive value on a test set. Liu et al. [154] examined the effectiveness of DL on full-field digital mammography in forecasting disease progression of BI-RADS 4 microcalcifications. Their collective DL solution surpassed clinical and DL image models, achieving high diagnostic accuracy. Moreover, it assisted junior radiologists in enhancing their performance. This study underscores the potential of DL in improving malignancy prediction in screening mammography and supporting clinical decision-making. A study explored the use of CNNs to predict whether patients diagnosed with pure atypical ductal hyperplasia (ADH) could be safely monitored rather than undergoing surgery. By analyzing 298 mammographic images from 149 patients, the AUC (ROC) was found to be 0.86. The findings suggest the feasibility of distinguishing ADH from DCIS [155].

Recently, Prodan et al. [156] explored DL methods, incorporating CNN and ViT architectures, to analyze mammograms with the goal of enhancing classification accuracy. They suggested an alternative data enhancement method using simulations to increase model accuracy and emphasized the importance of careful data preprocessing. Furthermore, their study combined interpretable AI techniques, like class function mapping, to gain insight into the model decision-making method. Beuke et al. [157] developed a DL algorithm to detect and classify breast lesions in contrast-enhanced mammography (CEM) images. Collected retrospective disease data, trained DL, and handcrafted radiomic features to distinguish between benign and malignant lesions were developed. The results showed remarkable sensitivity in lesion detection and good diagnostic accuracy. Notably, the combined DL and manual radiomics models achieved a remarkable AUC (ROC), indicating an encouraging probability for accurately detecting malignant lesions depicted in CEM images. Pesapane et al. [158] developed an AI model to detect and characterize microcalcifications in mammograms and facilitate breast cancer screening. The model used three networks (AlexNet, ResNet18, and ResNet34) to find impressive sensitivity, specificity, and AUC for ROC curves in microcalcification detection and classification tasks. The results confirmed the exceptional performance of AlexNet, while ResNet18 and ResNet34 also showed encouraging results.

Similarly, Kumar et al. [159] focused on a DL-based model for breast cancer detection. When model performance was evaluated using metrics such as sensitivity, specificity, accuracy, and F-measure on benchmark datasets. It was found that the proposed models performed better than current

methods, assisted radiologists with diagnostic and classification accuracy, and highlighted potential improvements. Tsai et al. [160] proposed a multitask DL algorithm to predict extensive intraductal component (EIC) in breast cancer development. Using mammograms from 2010-2019, the three-stage DL model showed impressive performance, with AUC (ROC) values of 0.76 and 0.77 for EIC prediction in imaging and breast, respectively. This multitask paradigm facilitated the simultaneous classification of imaging findings and prediction of EIC, thereby showing the possibilities of DL algorithms in improving breast cancer diagnosis via mammography. A comprehensive comparison of evaluations of some more DL-based techniques is illustrated in Table 6.

D. PROBLEMS IN CURRENT RESEARCH PROGRESS

Mammography is a crucial tool for breast cancer detection, but despite its importance, there are limitations and challenges in the current research progress. Addressing these issues is crucial to advancing mammography research. Mammography may not detect cancer in its early stages when it's most treatable. Other problems include unnecessary biopsies (FPs) or missed detections (FNs) in case of incorrect mammography performance scores [155]. Another problem arises when different radiologists interpret the same mammogram differently leading to inconsistent diagnosis. Similarly, less effective mammography for women with dense breasts makes it harder to detect tumors. The ionizing radiation can be harmful in case of high radiation doses [165], [166]. The mammography equipment and expertise may not be readily available in all regions, particularly in low-resource areas. Integrating and analyzing data from various sources, such as imaging and genetics, can be challenging. Over and above, while AI and ML can enhance mammography, they also have limitations and potential biases. Ensuring data privacy, informed consent, and regulatory compliance are essential but can be complex [166].

E. RESEARCH DIRECTIONS IN MAMMOGRAPHY

Artificial intelligence (AI) is expected to become an integral component of mammography screening, enabling radiologists to leverage AI-driven insights for more accurate and earlier detection of breast cancer, leading to improved patient outcomes and enhanced personalized care. The increased efficiency of radiologists using AI can result in decreased turnaround times. AI can be utilized for breast density assessment, which is associated with breast cancer risk [167]. Changes in breast density over time can be evaluated with AI and used as a biomarker for treatment response. AI based breast density algorithms can be integrated with other mammographic features, age, genetic data, and clinical factors to develop a risk prediction model for risk stratification, which can be incorporated into a clinical decision support system. DL models that accurately exclude cancer on mammograms can reduce radiologists' workload and be applied in underserved areas where breast imaging expertise

is limited [168]. The widespread acceptance of AI models can be facilitated by demonstrating their generalizability and validation on large, diverse populations, multiple vendors, and imaging acquisition techniques in extensive retrospective studies. The higher specificity of AI based computer-aided detection (CAD) compared to older non-AI CAD models and its potential to decrease recall rates, increase cancer detection rates, and enhance overall performance by improving these metrics [169].

IV. CONCLUSION

This study examines breast cancer detection via mammography over a specific period, aligning with multiple UN Sustainable Development Goals. Timely detection through screening has decreased mortality rates and potentially saved lives. Despite numerous review articles on mammographic breast cancer screening, there remains a gap for a focused review covering breast cancer detection from 1970 to 2023, emphasizing IP, ML, and DL. While ML has laid the foundation for image analysis in mammography, utilizing DL architectures with multi-scale feature extraction that transforms contextual information into feature data has yielded exceptional outcomes. While DL algorithms for breast cancer detection are increasingly being applied clinically, broader integration into mammogram-based cancer detection in clinical settings calls for additional clinical validation, enhanced reliability, generalizability, and interpretability, among other considerations.

REFERENCES

[1] *WHO Position Paper on Mammography Screening*. World Health Org., Geneva, Switzerland, 2014.

[2] J. Ferlay, E. Steliarova-Foucher, J. Lortet-Tieulent, S. Rosso, J. W. W. Coebergh, H. Comber, D. Forman, and F. Bray, "Cancer incidence and mortality patterns in Europe: Estimates for 40 countries in 2012," *Eur. J. Cancer*, vol. 49, no. 6, pp. 1374–1403, Apr. 2013.

[3] F. Biermann, N. Kanie, and R. E. Kim, "Global governance by goal-setting: The novel approach of the UN sustainable development goals," *Current Opinion Environ. Sustainability*, vols. 26–27, pp. 26–31, Jun. 2017.

[4] S. A. Feig, "Mammographic evaluation of calcifications," *RSNA Categorial Course Breast Imag.*, vol. 12, pp. 93–105, Jan. 1995.

[5] M. Muttarak, P. Kongmebhol, and N. Sukhamwang, "Breast calcifications: Which are malignant," *Singap. Med. J.*, vol. 50, no. 9, pp. 907–914, 2009.

[6] D. P. Winchester, J. M. Jeske, and R. Goldschmidt, "The diagnosis and management of ductal carcinoma in-situ of the breast," *CA, A Cancer J. Clinicians*, vol. 50, no. 3, pp. 184–200, May 2000.

[7] J. J. Fenton, S. H. Taplin, P. A. Carney, L. Abraham, E. A. Sickles, C. J. D'Orsi, E. A. Berns, G. Cutter, R. E. Hendrick, W. E. Barlow, and J. G. Elmore, "Influence of computer-aided detection on performance of screening mammography," *New England J. Med.*, vol. 356, no. 14, pp. 1399–1409, Apr. 2007.

[8] J. Wang, X. Yang, H. Cai, W. Tan, C. Jin, and L. Li, "Discrimination of breast cancer with microcalcifications on mammography by deep learning," *Sci. Rep.*, vol. 6, no. 1, p. 27327, Jun. 2016.

[9] C. F. Cowell, B. Weigelt, R. A. Sakr, C. K. Y. Ng, J. Hicks, T. A. King, and J. S. Reis-Filho, "Progression from ductal carcinoma in situ to invasive breast cancer: Revisited," *Mol. Oncol.*, vol. 7, no. 5, pp. 859–869, Oct. 2013.

[10] P. Rosen, R. E. Snyder, F. W. Foote, and T. Wallace, "Detection of occult carcinoma in the apparently benign breast biopsy through specimen radiography," *Cancer*, vol. 26, no. 4, pp. 944–952, Oct. 1970.

[11] J. A. Harvey, B. T. Nicholson, and M. A. Cohen, "Finding early invasive breast cancers: A practical approach," *Radiology*, vol. 248, no. 1, pp. 61–76, Jul. 2008.

[12] L. Tabár, S. W. Duffy, B. Viták, C. Chen, and T. C. Prevost, "The natural history of breast carcinoma: What have we learned from screening?" *Cancer*, vol. 86, no. 3, pp. 449–62, Aug. 1999.

[13] V. K. Singh, H. A. Rashwan, S. Romani, F. Akram, N. Pandey, M. M. K. Sarker, A. Saleh, M. Arenas, M. Arquez, D. Puig, and J. Torrents-Barrena, "Breast tumor segmentation and shape classification in mammograms using generative adversarial and convolutional neural network," *Exp. Syst. Appl.*, vol. 139, Jan. 2020, Art. no. 112855.

[14] P. Jaglan, R. Dass, and M. Duhan, "Breast cancer detection techniques: Issues and challenges," *J. Inst. Eng. (India), Ser. B*, vol. 100, no. 4, pp. 379–386, Aug. 2019.

[15] D. Ribli, A. Horváth, Z. Unger, P. Pollner, and I. Csabai, "Detecting and classifying lesions in mammograms with deep learning," *Sci. Rep.*, vol. 8, no. 1, p. 4165, Mar. 2018.

[16] K. C. Oeffinger, E. T. Fontham, R. Etzioni, A. Herzig, J. S. Michaelson, Y.-C. T. Shih, L. C. Walter, T. R. Church, C. R. Flowers, and S. J. LaMonte, "Breast cancer screening for women at average risk: 2015 guideline update from the American cancer society," *Jama*, vol. 314, no. 15, pp. 1599–1614, 2015.

[17] M. S. Bae, W. K. Moon, J. M. Chang, H. R. Koo, W. H. Kim, N. Cho, A. Yi, B. La Yun, S. H. Lee, M. Y. Kim, E. B. Ryu, and M. Seo, "Breast cancer detected with screening US: Reasons for nondetection at mammography," *Radiology*, vol. 270, no. 2, pp. 369–377, Feb. 2014.

[18] Y. LeCun, Y. Bengio, and G. Hinton, "Deep learning," *Nature*, vol. 521, no. 7553, pp. 436–444, 2015.

[19] S. S. Aboutalib, A. A. Mohamed, W. A. Berg, M. L. Zuley, J. H. Sumkin, and S. Wu, "Deep learning to distinguish recalled but benign mammography images in breast cancer screening," *Clin. Cancer Res.*, vol. 24, no. 23, pp. 5902–5909, Dec. 2018.

[20] E.-K. Kim, H.-E. Kim, K. Han, B. J. Kang, Y.-M. Sohn, O. H. Woo, and C. W. Lee, "Applying data-driven imaging biomarker in mammography for breast cancer screening: Preliminary study," *Sci. Rep.*, vol. 8, no. 1, p. 2762, Feb. 2018.

[21] A. Hamidinekoo, E. Denton, A. Rampun, K. Honnor, and R. Zwiggelaar, "Deep learning in mammography and breast histology, an overview and future trends," *Med. Image Anal.*, vol. 47, pp. 45–67, Jul. 2018.

[22] J. R. Burt, N. Torosdagli, N. Khosravan, H. RaviPrakash, A. Mortazi, F. Tissavirasingham, S. Hussein, and U. Bagci, "Deep learning beyond cats and dogs: Recent advances in diagnosing breast cancer with deep neural networks," *Brit. J. Radiol.*, vol. 91, no. 1089, Apr. 2018, Art. no. 20170545.

[23] T. Kooi, G. Litjens, B. V. Ginneken, A. Gubern-Mérida, C. I. Sánchez, R. M. Mann, A. D. Heeten, and N. Karssemeijer, "Large scale deep learning for computer aided detection of mammographic lesions," *Med. Image Anal.*, vol. 35, pp. 303–312, Aug. 2017.

[24] R. Agarwal, O. Diaz, X. Lladó, M. H. Yap, and R. Martí, "Automatic mass detection in mammograms using deep convolutional neural networks," *J. Med. Imag.*, vol. 6, no. 3, Feb. 2019, Art. no. 031409.

[25] S. Jeyasingh and M. Veluchamy, "Modified bat algorithm for feature selection with the Wisconsin diagnosis breast cancer (WDBC) dataset," *Asian Pacific J. Cancer Prevention, APJCP*, vol. 18, no. 5, pp. 1257–1264, May 2017.

[26] T. R. Mahesh, V. V. Kumar, V. Vivek, K. M. K. Raghunath, and G. S. Madhuri, "Early predictive model for breast cancer classification using blended ensemble learning," *Int. J. Syst. Assurance Eng. Manage.*, vol. 15, no. 1, pp. 188–197, Jan. 2024.

[27] S. Zhou, C. Hu, S. Wei, and X. Yan, "Breast cancer prediction based on multiple machine learning algorithms," *Technol. Cancer Res. Treatment*, vol. 23, Jan. 2024, Art. no. 15330338241234791.

[28] T. Islam, M. A. Sheakh, M. S. Tahosin, M. H. Hena, S. Akash, Y. A. Bin Jardan, G. FentahunWondmie, H.-A. Nafidi, and M. Bourhia, "Predictive modeling for breast cancer classification in the context of Bangladeshi patients by use of machine learning approach with explainable AI," *Sci. Rep.*, vol. 14, no. 1, p. 8487, Apr. 2024.

[29] S. Ünalan, O. Günay, I. Akkurt, K. Gunoglu, and H. O. Tekin, "A comparative study on breast cancer classification with stratified shuffle split and K-fold cross validation via ensembled machine learning," *J. Radiat. Res. Appl. Sci.*, vol. 17, no. 4, Dec. 2024, Art. no. 101080.

[30] D. Abdelhafiz, C. Yang, R. Ammar, and S. Nabavi, "Deep convolutional neural networks for mammography: Advances, challenges and applications," *BMC Bioinf.*, vol. 20, no. 11, pp. 1–20, Jun. 2019.

[31] S. J. S. Gardezi, A. Elazab, B. Lei, and T. Wang, "Breast cancer detection and diagnosis using mammographic data: Systematic review," *J. Med. Internet Res.*, vol. 21, no. 7, Jul. 2019, Art. no. e14464.

[32] K. J. Geras, R. M. Mann, and L. Moy, "Artificial intelligence for mammography and digital breast tomosynthesis: Current concepts and future perspectives," *Radiology*, vol. 293, no. 2, pp. 246–259, Nov. 2019.

[33] S. E. Hickman, R. Woitek, E. P. V. Le, Y. R. Im, C. M. Luxhøj, A. I. Aviles-Rivero, G. C. Baxter, J. W. MacKay, and F. J. Gilbert, "Machine learning for workflow applications in screening mammography: Systematic review and meta-analysis," *Radiology*, vol. 302, no. 1, pp. 88–104, Jan. 2022.

[34] N. Khan, R. Adam, P. Huang, T. Maldjian, and T. Q. Duong, "Deep learning prediction of pathologic complete response in breast cancer using MRI and other clinical data: A systematic review," *Tomography*, vol. 8, no. 6, pp. 2784–2795, Nov. 2022.

[35] A. Verbeek, R. Holland, F. Sturmans, J. Hendriks, M. Avunac, and N. Day, "Reduction of breast cancer mortality through mass screening with modern mammography: First results of the Nijmegen project, 1975–1981," *Lancet*, vol. 323, no. 8388, pp. 1222–1224, 1984.

[36] J. Wolfe, A. Saftlas, and M. Salane, "Mammographic parenchymal patterns and quantitative evaluation of mammographic densities: A case-control study," *Amer. J. Roentgenol.*, vol. 148, no. 6, pp. 1087–1092, Jun. 1987.

[37] P. A. Carney, D. L. Miglioretti, B. C. Yankaskas, K. Kerlikowske, R. Rosenberg, C. M. Rutter, B. M. Geller, L. A. Abraham, S. H. Taplin, M. Dignan, G. Cutter, and R. Ballard-Barbash, "Individual and combined effects of age, breast density, and hormone replacement therapy use on the accuracy of screening mammography," *Ann. Internal Med.*, vol. 138, no. 3, p. 168, Feb. 2003.

[38] E. Warner, D. B. Plewes, K. A. Hill, P. A. Causer, J. T. Zubovits, R. A. Jong, M. R. Cutrara, G. DeBoer, M. J. Yaffe, and S. J. Messner, "Surveillance of BRCA1 and BRCA2 mutation carriers with magnetic resonance imaging, ultrasound, mammography, and clinical breast examination," *Jama*, vol. 292, no. 11, pp. 1317–1325, 2004.

[39] L. Tarassenko, "Novelty detection for the identification of masses in mammograms," in *Proc. 4th Int. Conf. Artif. Neural Netw.*, 1995, pp. 442–447.

[40] D. Saslow, C. Boetes, W. Burke, S. Harms, M. O. Leach, C. D. Lehman, E. Morris, E. Pisano, M. Schnall, S. Sener, R. A. Smith, E. Warner, M. Yaffe, K. S. Andrews, and C. A. Russell, "American cancer society guidelines for breast screening with MRI as an adjunct to mammography," *CA, A Cancer J. Clinicians*, vol. 57, no. 2, pp. 75–89, Mar. 2007.

[41] M. Jiang, S. Zhang, H. Li, and D. N. Metaxas, "Computer-aided diagnosis of mammographic masses using scalable image retrieval," *IEEE Trans. Biomed. Eng.*, vol. 62, no. 2, pp. 783–792, Feb. 2015.

[42] J. Dheeba, N. A. Singh, and S. Tamil Selvi, "Computer-aided detection of breast cancer on mammograms: A swarm intelligence optimized wavelet neural network approach," *J. Biomed. Informat.*, vol. 49, pp. 45–52, Jun. 2014.

[43] H. G. Welch, P. C. Prorok, A. J. O'Malley, and B. S. Kramer, "Breast-cancer tumor size, overdiagnosis, and mammography screening effectiveness," *New England J. Med.*, vol. 375, no. 15, pp. 1438–1447, Oct. 2016.

[44] W. Xie, Y. Li, and Y. Ma, "Breast mass classification in digital mammography based on extreme learning machine," *Neurocomputing*, vol. 173, pp. 930–941, Jan. 2016.

[45] R. M. Rangayyan, L. Shen, Y. Shen, J. E. L. Desautels, H. Bryant, T. J. Terry, N. Horeczko, and M. S. Rose, "Improvement of sensitivity of breast cancer diagnosis with adaptive neighborhood contrast enhancement of mammograms," *IEEE Trans. Inf. Technol. Biomed.*, vol. 1, no. 3, pp. 161–170, Sep. 1997.

[46] J. Tang, X. Liu, and Q. Sun, "A direct image contrast enhancement algorithm in the wavelet domain for screening mammograms," *IEEE J. Sel. Topics Signal Process.*, vol. 3, no. 1, pp. 74–80, Feb. 2009.

[47] C. Wang and Z. Ye, "Brightness preserving histogram equalization with maximum entropy: A variational perspective," *IEEE Trans. Consum. Electron.*, vol. 51, no. 4, pp. 1326–1334, Nov. 2005.

[48] Y. Zhao, N. D. Georganas, and E. M. Petriu, "Applying contrast-limited adaptive histogram equalization and integral projection for facial feature enhancement and detection," in *IEEE Instrum. Meas. Technol. Conf. Proc.*, May 2010, pp. 861–866.

[49] R. Gordon and R. M. Rangayyan, "Feature enhancement of film mammograms using fixed and adaptive neighborhoods," *Appl. Opt.*, vol. 23, no. 4, pp. 560–564, 1984.

[50] F. Sofos, D. Drikakis, and I. W. Kokkinakis, "Deep learning architecture for sparse and noisy turbulent flow data," *Phys. Fluids*, vol. 36, no. 3, Mar. 2024, Art. no. 035155.

[51] F. Sofos, D. Drikakis, and I. W. Kokkinakis, "Comparison of super-resolution deep learning models for flow imaging," *Comput. Fluids*, vol. 283, Oct. 2024, Art. no. 106396.

[52] F. Sofos, D. Drikakis, I. W. Kokkinakis, and S. M. Spottswood, "A deep learning super-resolution model for turbulent image upscaling and its application to shock wave–boundary layer interaction," *Phys. Fluids*, vol. 36, no. 2, Feb. 2024, Art. no. 025117.

[53] K. Poulinakis, D. Drikakis, I. W. Kokkinakis, and S. M. Spottswood, "Machine-learning methods on noisy and sparse data," *Mathematics*, vol. 11, no. 1, p. 236, Jan. 2023.

[54] F. Sofos, D. Drikakis, I. W. Kokkinakis, and S. M. Spottswood, "Convolutional neural networks for compressible turbulent flow reconstruction," *Phys. Fluids*, vol. 35, no. 11, Nov. 2023, Art. no. 116120.

[55] L. Zhang, W. Qian, R. Sankar, D. Song, and R. Clark, "A new false positive reduction method for MCCs detection in digital mammography," in *Proc. IEEE Int. Conf. Acoust., Speech, Signal Process.*, vol. 2, May 2001, pp. 1033–1036.

[56] D. H. Davies and D. R. Dance, "Automatic computer detection of clustered calcifications in digital mammograms," *Phys. Med. Biol.*, vol. 35, no. 8, pp. 1111–1118, Aug. 1990.

[57] J. Kook Kim and H. Wook Park, "Statistical textural features for detection of microcalcifications in digitized mammograms," *IEEE Trans. Med. Imag.*, vol. 18, no. 3, pp. 231–238, Mar. 1999.

[58] R. M. Haralick, K. Shanmugam, and I. Dinstein, "Textural features for image classification," *IEEE Trans. Syst., Man, Cybern.*, vol. SMC-3, no. 6, pp. 610–621, Nov. 1973.

[59] M. M. Galloway, "Texture analysis using gray level run lengths," *Comput. Graph. Image Process.*, vol. 4, no. 2, pp. 172–179, Jun. 1975.

[60] J. S. Weszka, C. R. Dyer, and A. Rosenfeld, "A comparative study of texture measures for terrain classification," *IEEE Trans. Syst., Man, Cybern.*, vol. SMC-6, no. 4, pp. 269–285, Apr. 1976.

[61] N. H. Eltonsy, G. D. Tourassi, and A. S. Elmaghraby, "A concentric morphology model for the detection of masses in mammography," *IEEE Trans. Med. Imag.*, vol. 26, no. 6, pp. 880–889, Jun. 2007.

[62] K. I. Laws, "Textured image segmentation," Univ. Southern California, Tech. Rep. 7293879, 1981. [Online]. Available: https://elibrary.ru/item.asp?id=7293879

[63] S. Yu, L. Guan, and S. Brown, "Automatic detection of clustered microcalcifications in digitized mammogram films," *J. Electron. Imag.*, vol. 8, no. 1, pp. 76–82, 1999.

[64] A. P. Dhawan, Y. Chitre, and C. Kaiser-Bonasso, "Analysis of mammographic microcalcifications using gray-level image structure features," *IEEE Trans. Med. Imag.*, vol. 15, no. 3, pp. 246–259, Jun. 1996.

[65] F. R. Rad, H. Soltanian-Zadeh, M. Rahmati, and S. Pour-Abdollah, "Microcalcification classification in mammograms using multiwavelet features," *Proc. SPIE*, vol. 3813, pp. 832–841, Oct. 1999.

[66] G. L. Rogova, P. C. Stomper, and C.-C. Ke, "Microcalcification texture analysis in a hybrid system for computer-aided mammography," *Proc. SPIE*, vol. 3661, pp. 1426–1433, May 1999.

[67] T. Netsch and H.-O. Peitgen, "Scale-space signatures for the detection of clustered microcalcifications in digital mammograms," *IEEE Trans. Med. Imag.*, vol. 18, no. 9, pp. 774–786, Sep. 1999.

[68] H. D. Cheng, X. Cai, X. Chen, L. Hu, and X. Lou, "Computer-aided detection and classification of microcalcifications in mammograms: A survey," *Pattern Recognit.*, vol. 36, no. 12, pp. 2967–2991, Dec. 2003.

[69] N. Alpaslan, A. Kara, B. Zencir, and D. Hanbay, "Classification of breast masses in mammogram images using KNN," in *Proc. 23rd Signal Process. Commun. Appl. Conf. (SIU)*, May 2015, pp. 1469–1472.

[70] J. Kamalakannan and M. R. Babu, "Classification of breast abnormality using decision tree based on GLCM features in mammograms," *Int. J. Comput. Aided Eng. Technol.*, vol. 10, no. 5, pp. 504–512, 2018.

[71] T. M. Mitchell and T. M. Mitchell, *Machine Learning*, vol. 1, no. 9. New York, NY, USA: McGraw-Hill, 1997.

[72] S. Krishnaveni, R. Bhanumathi, and T. Pugazharasan, "Study of mammogram microcalcification to aid tumour detection using naive Bayes classifier," *Int. J. Adv. Res. Electr., Electron. Instrum. Eng.*, vol. 3, no. 3, p. 8274, 2014.

[73] J. D. M. Rennie, L. Shih, J. Teevan, and D. R. Karger, "Tackling the poor assumptions of naive Bayes text classifiers," in *Proc. 20th Int. Conf. Mach. Learn.*, Aug. 2003, pp. 616–623.

[74] A. T. Azar and S. A. El-Said, "Performance analysis of support vector machines classifiers in breast cancer mammography recognition," *Neural Comput. Appl.*, vol. 24, no. 5, pp. 1163–1177, Apr. 2014.

[75] E. Alpaydin, *Introduction To Machine Learning*. Cambridge, MA, USA: MIT Press, 2020.

[76] A. Krizhevsky, I. Sutskever, and G. E. Hinton, "ImageNet classification with deep convolutional neural networks," in *Proc. Adv. Neural Inf. Process. Syst.*, vol. 25, 2012, pp. 1–9.

[77] A. Arokiyamary Delphina, M. Kamarasan, and S. Sathiamoorthy, "Image processing for identification of breast cancer: A literature survey," *Asian J. Electr. Sci.*, vol. 7, no. 2, pp. 28–37, Nov. 2018.

[78] L. Lyons, *Statistical Problems in Particle Physics, Astrophysics and Cosmology*. Oxford, U.K.: Imperial College Press, Sep. 2005, pp. 12–15.

[79] D. F. Specht, "Probabilistic neural networks," *Neural Netw.*, vol. 3, no. 1, pp. 109–118, Jan. 1990.

[80] B. Zheng, W. Qian, and L. P. Clarke, "Digital mammography: Mixed feature neural network with spectral entropy decision for detection of microcalcifications," *IEEE Trans. Med. Imag.*, vol. 15, no. 5, pp. 589–597, Oct. 1996.

[81] A.-A. Nahid and Y. Kong, "Involvement of machine learning for breast cancer image classification: A survey," *Comput. Math. Methods Med.*, vol. 2017, pp. 1–29, Jan. 2017.

[82] A. Bhandare, M. Bhide, P. Gokhale, and R. Chandavarkar, "Applications of convolutional neural networks," *Int. J. Comput. Sci. Inf. Technol.*, vol. 7, no. 5, pp. 2206–2215, 2016.

[83] B. Sahiner, H.-P. Chan, N. Petrick, D. Wei, M. A. Helvie, D. D. Adler, and M. M. Goodsitt, "Classification of mass and normal breast tissue: A convolution neural network classifier with spatial domain and texture images," *IEEE Trans. Med. Imag.*, vol. 15, no. 5, pp. 598–610, Oct. 1996.

[84] S.-C. B. Lo, H. Li, Y. Wang, L. Kinnard, and M. T. Freedman, "A multiple circular path convolution neural network system for detection of mammographic masses," *IEEE Trans. Med. Imag.*, vol. 21, no. 2, pp. 150–158, Feb. 2002.

[85] P. Fonseca, J. Mendoza, J. Wainer, J. Ferrer, J. A. Pinto, J. Guerrero, and B. Castañeda, "Automatic breast density classification using a convolutional neural network architecture search procedure," *Proc. SPIE*, vol. 9414, Mar. 2015, Art. no. 941428.

[86] H. Su, F. Liu, Y. Xie, F. Xing, S. Meyyappan, and L. Yang, "Region segmentation in histopathological breast cancer images using deep convolutional neural network," in *Proc. IEEE 12th Int. Symp. Biomed. Imag. (ISBI)*, Apr. 2015, pp. 55–58.

[87] Z. Jiao, X. Gao, Y. Wang, and J. Li, "A deep feature based framework for breast masses classification," *Neurocomputing*, vol. 197, pp. 221–231, Jul. 2016.

[88] J. Arevalo, F. A. González, R. Ramos-Pollán, J. L. Oliveira, and M. A. G. Lopez, "Representation learning for mammography mass lesion classification with convolutional neural networks," *Comput. Methods Programs Biomed.*, vol. 127, pp. 248–257, Apr. 2016.

[89] H. Rezaeilouyeh, A. Mollahosseini, and M. H. Mahoor, "Microscopic medical image classification framework via deep learning and shearlet transform," *J. Med. Imag.*, vol. 3, no. 4, Nov. 2016, Art. no. 044501.

[90] M. M. Jadoon, Q. Zhang, I. U. Haq, S. Butt, and A. Jadoon, "Three-class mammogram classification based on descriptive CNN features," *BioMed Res. Int.*, vol. 2017, pp. 1–11, Jan. 2017.

[91] M. Arfan, "Deep learning based computer aided diagnosis system for breast mammograms," *Int. J. Adv. Comput. Sci. Appl.*, vol. 8, no. 7, pp. 286–290, 2017.

[92] W. Zhu, X. Xiang, T. D. Tran, G. D. Hager, and X. Xie, "Adversarial deep structured nets for mass segmentation from mammograms," in *Proc. IEEE 15th Int. Symp. Biomed. Imag. (ISBI)*, Apr. 2018, pp. 847–850.

[93] H. Wang, J. Feng, Z. Zhang, H. Su, L. Cui, H. He, and L. Liu, "Breast mass classification via deeply integrating the contextual information from multi-view data," *Pattern Recognit.*, vol. 80, pp. 42–52, Aug. 2018.

[94] A. Gastounioti, A. Oustimov, M.-K. Hsieh, L. Pantalone, E. F. Conant, and D. Kontos, "Using convolutional neural networks for enhanced capture of breast parenchymal complexity patterns associated with breast cancer risk," *Academic Radiol.*, vol. 25, no. 8, pp. 977–984, Aug. 2018.

[95] J.-Y. Chiao, K.-Y. Chen, K. Y.-K. Liao, P.-H. Hsieh, G. Zhang, and T.-C. Huang, "Detection and classification the breast tumors using mask R-CNN on sonograms," *Medicine*, vol. 98, no. 19, 2019, Art. no. e15200.

[96] S. Hochreiter, "Long short-term memory," in *Neural Computation*. Cambridge, MA, USA: MIT Press, 1997.

[97] A.-A. Nahid, M. A. Mehrabi, and Y. Kong, "Histopathological breast cancer image classification by deep neural network techniques guided by local clustering," *BioMed Res. Int.*, vol. 2018, no. 1, 2018, Art. no. 2362108.

[98] J. Suckling, J. Parker, D. Dance, S. Astley, I. Hutt, C. Boggis, I. Ricketts, E. Stamatakis, N. Cerneaz, and S. Kok, "Mammographic image analysis society (MIAS) database v1. 21," Apollo Univ. Cambridge Repository, Tech. Rep., 2015. [Online]. Available: https://doi.org/10.17863/CAM.105113

[99] J. Suckling, "The mammographic images analysis society digital mammogram database," in *Proc. Exerpta Medica. Int. Congr. Ser.*, vol. 1069, Jan. 1994, pp. 375–378.

[100] M. Heath, K. Bowyer, D. Kopans, P. Kegelmeyer Jr., R. Moore, K. Chang, and S. Munishkumaran, "Current status of the digital database for screening mammography," in *Digital Mammography*. Berlin, Germany: Springer, 1998, pp. 457–460.

[101] R. S. Lee, F. Gimenez, A. Hoogi, K. K. Miyake, M. Gorovoy, and D. L. Rubin, "A curated mammography data set for use in computer-aided detection and diagnosis research," *Sci. Data*, vol. 4, no. 1, pp. 1–9, Dec. 2017.

[102] J. E. Oliveira, M. O. Gueld, A. d. A. Araújo, B. Ott, and T. M. Deserno, "Toward a standard reference database for computer-aided mammography," *Proc. SPIE*, vol. 6915, pp. 606–614, Mar. 2008.

[103] B. R. N. Matheus and H. Schiabel, "Online mammographic images database for development and comparison of CAD schemes," *J. Digit. Imag.*, vol. 24, no. 3, pp. 500–506, Jun. 2011.

[104] I. C. Moreira, I. Amaral, I. Domingues, A. Cardoso, M. J. Cardoso, and J. S. Cardoso, "INbreast: Toward a full-field digital mammographic database," *Acad. Radiol.*, vol. 19, no. 2, pp. 236–248, 2012.

[105] A. S. Alsolami, W. Shalash, W. Alsaggaf, S. Ashoor, H. Refaat, and M. Elmogy, "King abdulaziz university breast cancer mammogram dataset (KAU-BCMD)," *Data*, vol. 6, no. 11, p. 111, Oct. 2021.

[106] H. T. Nguyen, H. Q. Nguyen, H. H. Pham, K. Lam, L. T. Le, M. Dao, and V. Vu, "VinDr-mammo: A large-scale benchmark dataset for computer-aided diagnosis in full-field digital mammography," *Sci. Data*, vol. 10, no. 1, p. 277, May 2023.

[107] H. H. Pham, H. N. Trung, and H. Q. Nguyen, "Vindr-mammo: A large-scale benchmark dataset for computer-aided detection and diagnosis in full-field digital mammography," *Sci Data*, 2022. [Online]. Available: https://doi.org/10.13026/br2v-7517

[108] T. Matsubara, "Development of mass detection algorithm based on adaptive thresholding technique in digital mammograms," in *Proc. Digital Mammography*, 1996, pp. 391–396.

[109] A. Rojas Domínguez and A. K. Nandi, "Detection of masses in mammograms via statistically based enhancement, multilevel-thresholding segmentation, and region selection," *Computerized Med. Imag. Graph.*, vol. 32, no. 4, pp. 304–315, Jun. 2008.

[110] V. A. Karale, J. P. Ebenezer, J. Chakraborty, T. Singh, A. Sadhu, N. Khandelwal, and S. Mukhopadhyay, "A screening CAD tool for the detection of microcalcification clusters in mammograms," *J. Digit. Imag.*, vol. 32, no. 5, pp. 728–745, Oct. 2019.

[111] F. Zhang, L. Luo, X. Sun, Z. Zhou, X. Li, Y. Yu, and Y. Wang, "Cascaded generative and discriminative learning for microcalcification detection in breast mammograms," in *Proc. IEEE/CVF Conf. Comput. Vis. Pattern Recognit. (CVPR)*, Jun. 2019, pp. 12570–12578.

[112] V. A. Karale, T. Singh, A. Sadhu, N. Khandelwal, and S. Mukhopadhyay, "Reduction of false positives in the screening CAD tool for microcalcification detection," *Sādhanā*, vol. 45, no. 1, pp. 1–11, Dec. 2020.

[113] V. A. Karale, S. Mukhopadhyay, T. Singh, N. Khandelwal, and A. Sadhu, "Automated detection of microcalcification clusters in mammograms," in *Medical Imaging 2017: Computer-Aided Diagnosis*, 2017, Paper 101342R.

[114] B. Zheng, C. Mello-Thoms, X.-H. Wang, and D. Gur, "Improvement of visual similarity of similar breast masses selected by computer-aided diagnosis schemes," in *Proc. 4th IEEE Int. Symp. Biomed. Imag., From Nano Macro*, Apr. 2007, pp. 516–519.

[115] F. Zou, Y. Zheng, Z. Zhou, and K. Agyepong, "Gradient vector flow field and mass region extraction in digital mammograms," in *Proc. 21st IEEE Int. Symp. Computer-Based Med. Syst.*, Jun. 2008, pp. 41–43.

[116] Y. Yuan, M. L. Giger, H. Li, and C. A. Sennett, "Correlative feature analysis of FFDM images," *Proc. SPIE*, vol. 6915, pp. 497–502, Mar. 2008.

[117] A. E. Hassanien and J. M. Ali, "Digital mammogram segmentation algorithm using pulse coupled neural networks," in *Proc. 3rd Int. Conf. Image Graph. (ICIG)*, 2004, pp. 92–95.

[118] C. B. Caldwell, S. J. Stapleton, D. W. Holdsworth, R. A. Jong, W. J. Weiser, G. Cooke, and M. J. Yaffe, "Characterisation of mammographic parenchymal pattern by fractal dimension," *Phys. Med. Biol.*, vol. 35, no. 2, pp. 235–247, Feb. 1990.

[119] B. Zheng, Y.-H. Chang, X. H. Wang, W. F. Good, and D. Gur, "Application of a Bayesian belief network in a computer-assisted diagnosis scheme for mass detection," *Proc. SPIE*, vol. 3661, pp. 1553–1561, May 1999.

[120] D. Kramer and F. Aghdasi, "Texture analysis techniques for the classification of microcalcifications in digitised mammograms," in *Proc. IEEE Africon. 5th Africon Conf. Afr.*, vol. 1, Sep. 1999, pp. 395–400.

[121] K. Cao, F. Gao, R. Long, F.-D. Zhang, C.-C. Huang, M. Cao, Y.-Z. Yu, and Y.-S. Sun, "Peri-lesion regions in differentiating suspicious breast calcification-only lesions specifically on contrast enhanced mammography," *J. X-Ray Sci. Technol.*, pp. 1–14, Jan. 2024.

[122] F. Prinzi, A. Orlando, S. Gaglio, and S. Vitabile, "Interpretable radiomic signature for breast microcalcification detection and classification," *J. Imag. Informat. Med.*, vol. 37, no. 3, pp. 1038–1053, Feb. 2024.

[123] H. Yoen, M.-J. Jang, A. Yi, W. K. Moon, and J. M. Chang, "Artificial intelligence for breast cancer detection on mammography: Factors related to cancer detection," *Academic Radiol.*, vol. 31, no. 6, pp. 2239–2247, Jun. 2024.

[124] A. A. Malek, M. A. Alias, F. A. Razak, M. S. M. Noorani, R. Mahmud, and N. F. S. Zulkepli, "Persistent homology-based machine learning method for filtering and classifying mammographic microcalcification images in early cancer detection," *Cancers*, vol. 15, no. 9, p. 2606, May 2023.

[125] A. Khalid, A. Mehmood, A. Alabrah, B. F. Alkhamees, F. Amin, H. AlSalman, and G. S. Choi, "Breast cancer detection and prevention using machine learning," *Diagnostics*, vol. 13, no. 19, p. 3113, Oct. 2023.

[126] L. Li, W. Qian, L. P. Clarke, R. A. Clark, and J. A. Thomas, "Improving mass detection by adaptive and multiscale processing in digitized mammograms," *Proc. SPIE*, vol. 3661, pp. 490–498, May 1999.

[127] I. Iseri and C. Oz, "Computer aided detection of microcalcification clusters in mammogram images with machine learning approach," *Optoelectron. Adv. Mater.*, vol. 8, pp. 689–695, Jan. 2014.

[128] A. Rampun, H. Wang, B. Scotney, P. Morrow, and R. Zwiggelaar, "Classification of mammographic microcalcification clusters with machine learning confidence levels," *Proc. SPIE*, vol. 10718, pp. 345–352, Jul. 2018.

[129] A. Fanizzi, T. M. A. Basile, L. Losurdo, R. Bellotti, U. Bottigli, R. Dentamaro, V. Didonna, A. Fausto, R. Massafra, M. Moschetta, O. Popescu, P. Tamborra, S. Tangaro, and D. La Forgia, "A machine learning approach on multiscale texture analysis for breast microcalcification diagnosis," *BMC Bioinf.*, vol. 21, no. 2, pp. 1–11, Mar. 2020.

[130] V. P. T. Vy, M. M.-S. Yao, N. Q. Khanh Le, and W. P. Chan, "Machine learning algorithm for distinguishing ductal carcinoma in situ from invasive breast cancer," *Cancers*, vol. 14, no. 10, p. 2437, May 2022.

[131] Z. M. Sarvestani, J. Jamali, M. Taghizadeh, and M. H. F. Dindarloo, "A novel machine learning approach on texture analysis for automatic breast microcalcification diagnosis classification of mammogram images," *J. Cancer Res. Clin. Oncol.*, vol. 149, no. 9, pp. 6151–6170, Aug. 2023.

[132] Q. Lin, W.-M. Tan, J.-Y. Ge, Y. Huang, Q. Xiao, Y.-Y. Xu, Y.-T. Jin, Z.-M. Shao, Y.-J. Gu, B. Yan, and K.-D. Yu, "Artificial intelligence-based diagnosis of breast cancer by mammography microcalcification," *Fundam. Res.*, Jun. 2023. [Online]. Available: https://doi.org/10.1016/j.fmre.2023.04.018

[133] J. C. Fu, S. K. Lee, S. T. C. Wong, J. Y. Yeh, A. H. Wang, and H. K. Wu, "Image segmentation feature selection and pattern classification for mammographic microcalcifications," *Computerized Med. Imag. Graph.*, vol. 29, no. 6, pp. 419–429, Sep. 2005.

[134] E. Golobardes, J. Martí, J. Español, M. S. Llorente, J. Freixenet, X. L. Fábrega, A. Maroto, and E. B. Mansilla, "Classifying microcalcifications in digital mammograms using machine learning techniques," in *Proc. 4rt Congrés Català d'Intel.ligència Artif.*, Barcelona, Spain, Oct. 2001.

[135] M. A. Alolfe, W. A. Mohamed, A.-B. M. Youssef, Y. M. Kadah, and A. S. Mohamed, "Feature selection in computer aided diagnostic system for microcalcification detection in digital mammograms," in *Proc. Nat. Radio Sci. Conf.*, 2009, pp. 1–9.

[136] A. Papadopoulos, D. I. Fotiadis, and A. Likas, "Characterization of clustered microcalcifications in digitized mammograms using neural networks and support vector machines," *Artif. Intell. Med.*, vol. 34, no. 2, pp. 141–150, Jun. 2005.

[137] C. Y. Wu, S.-C. B. Lo, M. T. Freedman, A. Hasegawa, R. A. Zuurbier, and S. K. Mun, "Classification of microcalcifications in radiographs of pathological specimen for the diagnosis of breast cancer," *Proc. SPIE*, vol. 2167, pp. 630–641, May 1994.

[138] B. Q. Huynh, H. Li, and M. L. Giger, "Digital mammographic tumor classification using transfer learning from deep convolutional neural networks," *J. Med. Imag.*, vol. 3, no. 3, Aug. 2016, Art. no. 034501.

[139] S. R. Sannasi Chakravarthy and H. Rajaguru, "Automatic detection and classification of mammograms using improved extreme learning machine with deep learning," *IRBM*, vol. 43, no. 1, pp. 49–61, Feb. 2022.

[140] D. Ueda, A. Yamamoto, T. Takashima, N. Onoda, S. Noda, S. Kashiwagi, T. Morisaki, S. Tsutsumi, T. Honjo, A. Shimazaki, T. Goto, and Y. Miki, "Visualizing 'featureless' regions on mammograms classified as invasive ductal carcinomas by a deep learning algorithm: The promise of AI support in radiology," *Japanese J. Radiol.*, vol. 39, no. 4, pp. 333–340, Apr. 2021.

[141] B. Swiderski, L. Gielata, P. Olszewski, S. Osowski, and M. Kołodziej, "Deep neural system for supporting tumor recognition of mammograms using modified GAN," *Exp. Syst. Appl.*, vol. 164, Feb. 2021, Art. no. 113968.

[142] C. Xu, M. Lou, Y. Qi, Y. Wang, J. Pi, and Y. Ma, "Multi-scale attention-guided network for mammograms classification," *Biomed. Signal Process. Control*, vol. 68, Jul. 2021, Art. no. 102730.

[143] M.-L. Huang and T.-Y. Lin, "Considering breast density for the classification of benign and malignant mammograms," *Biomed. Signal Process. Control*, vol. 67, May 2021, Art. no. 102564.

[144] S. A. Haider, S. M. Pressman, S. Borna, C. A. Gomez-Cabello, A. Sehgal, B. C. Leibovich, and A. J. Forte, "Evaluating large language model (LLM) performance on established breast classification systems," *Diagnostics*, vol. 14, no. 14, p. 1491, Jul. 2024.

[145] D. A. Zebari, D. A. Ibrahim, D. Q. Zeebaree, M. A. Mohammed, H. Haron, N. A. Zebari, R. Damaševičius, and R. Maskeliūnas, "Breast cancer detection using mammogram images with improved multi-fractal dimension approach and feature fusion," *Appl. Sci.*, vol. 11, no. 24, p. 12122, Dec. 2021.

[146] A. Nomani, Y. Ansari, M. H. Nasirpour, A. Masouman, E. S. Pour, and A. Valizadeh, "PSOWNNs-CNN: A computational radiology for breast cancer diagnosis improvement based on image processing using machine learning methods," *Comput. Intell. Neurosci.*, vol. 2022, pp. 1–17, May 2022.

[147] S. Maqsood, R. Damaševič ius, and R. Maskeliūnas, "TTCNN: A breast cancer detection and classification towards computer-aided diagnosis using digital mammography in early stages," *Appl. Sci.*, vol. 12, no. 7, p. 3273, Mar. 2022.

[148] R.-H. Lin, B. K. Kujabi, C.-L. Chuang, C.-S. Lin, and C.-J. Chiu, "Application of deep learning to construct breast cancer diagnosis model," *Appl. Sci.*, vol. 12, no. 4, p. 1957, Feb. 2022.

[149] S. Mohapatra, S. Muduly, S. Mohanty, J. V. R. Ravindra, and S. N. Mohanty, "Evaluation of deep learning models for detecting breast cancer using histopathological mammograms images," *Sustain. Oper. Comput.*, vol. 3, pp. 296–302, Jan. 2022.

[150] R. M. Al-Tam, A. M. Al-Hejri, S. M. Narangale, N. A. Samee, N. F. Mahmoud, M. A. Al-Masni, and M. A. Al-Antari, "A hybrid workflow of residual convolutional transformer encoder for breast cancer classification using digital X-ray mammograms," *Biomedicines*, vol. 10, no. 11, p. 2971, Nov. 2022.

[151] K. Kumar Singh, S. Kumar, M. Antonakakis, K. Moirogiorgou, A. Deep, K. L. Kashyap, M. K. Bajpai, and M. Zervakis, "Deep learning capabilities for the categorization of microcalcification," *Int. J. Environ. Res. Public Health*, vol. 19, no. 4, p. 2159, Feb. 2022.

[152] A. A. Alsheikhy, Y. Said, T. Shawly, A. K. Alzahrani, and H. Lahza, "Biomedical diagnosis of breast cancer using deep learning and multiple classifiers," *Diagnostics*, vol. 12, no. 11, p. 2863, Nov. 2022.

[153] K. Marathe, C. Marasinou, B. Li, N. Nakhaei, B. Li, J. G. Elmore, L. Shapiro, and W. Hsu, "Automated quantitative assessment of amorphous calcifications: Towards improved malignancy risk stratification," *Comput. Biol. Med.*, vol. 146, Jul. 2022, Art. no. 105504.

[154] H. Liu, Y. Chen, Y. Zhang, L. Wang, R. Luo, H. Wu, C. Wu, H. Zhang, W. Tan, H. Yin, and D. Wang, "A deep learning model integrating mammography and clinical factors facilitates the malignancy prediction of BI-RADS 4 microcalcifications in breast cancer screening," *Eur. Radiol.*, vol. 31, no. 8, pp. 5902–5912, Aug. 2021.

[155] R. Ha, S. Mutasa, E. P. V. Sant, J. Karcich, C. Chin, M. Z. Liu, and S. Jambawalikar, "Accuracy of distinguishing atypical ductal hyperplasia from ductal carcinoma in situ with convolutional neural network–based machine learning approach using mammographic image data," *Amer. J. Roentgenol.*, vol. 212, no. 5, pp. 1166–1171, May 2019.

[156] M. Prodan, E. Paraschiv, and A. Stanciu, "Applying deep learning methods for mammography analysis and breast cancer detection," *Appl. Sci.*, vol. 13, no. 7, p. 4272, Mar. 2023.

[157] M. P. L. Beuque, M. B. I. Lobbes, Y. van Wijk, Y. Widaatalla, S. Primakov, M. Majer, C. Balleyguier, H. C. Woodruff, and P. Lambin, "Combining deep learning and handcrafted radiomics for classification of suspicious lesions on contrast-enhanced mammograms," *Radiology*, vol. 307, no. 5, Jun. 2023, Art. no. 221843.

[158] F. Pesapane, C. Trentin, F. Ferrari, G. Signorelli, P. Tantrige, M. Montesano, C. Cicala, R. Virgoli, S. D'Acquisto, L. Nicosia, D. Origgi, and E. Cassano, "Deep learning performance for detection and classification of microcalcifications on mammography," *Eur. Radiol. Experim.*, vol. 7, no. 1, p. 69, Nov. 2023.

[159] S. Kumar, P. Bhambu, S. Pachar, J. C. Cotrina-Aliaga, and J. L. Arias-Gonzáles, "Deep learning-based computer-aided diagnosis model for the identification and classification of mammography images," *Social Netw. Comput. Sci.*, vol. 4, no. 5, p. 502, Jun. 2023.

[160] H.-Y. Tsai, Y.-W. Kao, J.-C. Wang, T.-Y. Tsai, W.-S. Chung, J.-S. Hsu, M.-F. Hou, and S.-F. Weng, "Multitask deep learning on mammography to predict extensive intraductal component in invasive breast cancer," *Eur. Radiol.*, vol. 34, no. 4, pp. 2593–2604, Oct. 2023.

[161] G. Carneiro, J. Nascimento, and A. P. Bradley, "Unregistered multiview mammogram analysis with pre-trained deep learning models," in *Proc. Int. Conf. Med. Image Comput. Comput.-Assist. Intervent.* Cham, Switzerland: Springer, 2015, pp. 652–660. [Online]. Available: https://doi.org/10.1007/978-3-319-24574-4_78

[162] W. Sun, T.-L. Tseng, J. Zhang, and W. Qian, "Enhancing deep convolutional neural network scheme for breast cancer diagnosis with unlabeled data," *Computerized Med. Imag. Graph.*, vol. 57, pp. 4–9, Apr. 2017.

[163] R. K. Samala, H.-P. Chan, L. M. Hadjiiski, K. Cha, and M. A. Helvie, "Deep-learning convolution neural network for computer-aided detection of microcalcifications in digital breast tomosynthesis," *Proc. SPIE*, vol. 9785, pp. 234–240, Mar. 2016.

[164] K. Alshamrani, H. A. Alshamrani, F. F. Alqahtani, and B. S. Almutairi, "Enhancement of mammographic images using histogram-based techniques for their classification using CNN," *Sensors*, vol. 23, no. 1, p. 235, Dec. 2022.

[165] S. Iranmakani, T. Mortezazadeh, F. Sajadian, M. F. Ghaziani, A. Ghafari, D. Khezerloo, and A. E. Musa, "A review of various modalities in breast imaging: Technical aspects and clinical outcomes," *Egyptian J. Radiol. Nucl. Med.*, vol. 51, no. 1, pp. 1–22, Dec. 2020.

[166] C. Reis, A. Pascoal, T. Sakellaris, and M. Koutalonis, "Quality assurance and quality control in mammography: A review of available guidance worldwide," *Insights into Imag.*, vol. 4, no. 5, pp. 539–553, Oct. 2013.

[167] A. T. Wang, C. M. Vachon, K. R. Brandt, and K. Ghosh, "Breast density and breast cancer risk: A practical review," *Mayo Clinic Proc.*, vol. 89, no. 4, pp. 548–557, 2014.

[168] A. Rodriguez-Ruiz, K. Lång, A. Gubern-Merida, J. Teuwen, M. Broeders, G. Gennaro, P. Clauser, T. H. Helbich, M. Chevalier, T. Mertelmeier, M. G. Wallis, I. Andersson, S. Zackrisson, I. Sechopoulos, and R. M. Mann, "Can we reduce the workload of mammographic screening by automatic identification of normal exams with artificial intelligence? A feasibility study," *Eur. Radiol.*, vol. 29, no. 9, pp. 4825–4832, Sep. 2019.

[169] M. Tartar, L. Le, A. T. Watanabe, and A. J. Enomoto, "Artificial intelligence support for mammography: In-practice clinical experience," *J. Amer. College Radiol.*, vol. 18, no. 11, pp. 1510–1513, Nov. 2021.

SHAHZAD AHMAD QURESHI received the B.Sc. degree in metallurgy and materials engineering from UET Lahore, Pakistan, the Post Graduate Diploma degree in computer systems from CTC, Pakistan, the first M.Sc. degree in computer science from AK University, Pakistan, the second M.Sc. degree in nuclear engineering from Quaid-i-Azam University (QAU), Islamabad, and the Ph.D. degree from Pakistan Institute of Engineering and Applied Sciences (PIEAS), Pakistan, in 2008.

He has been a Research Associate with the University of Warwick, U.K., during his Ph.D. study. Most recently, he has been a Professor with the Department of Computer and Information Sciences, PIEAS. Some projects completed are linked to acoustic signal processing, geosensing-based earthquake prediction, satellite, and hyperspectral imaging. His research interests include medical image analysis, deep learning, evolutionary computing, and computer vision on applications for solving problems related to breast cancer detection/segmentation, cell counting, prostate cancer, transmission tomography-based medical image reconstruction, retinopathy, He-La cervical cancer cells investigation, 3D-digital subtraction angiography, and brain disorders (Parkinson's disease, Epilepsy, Alzheimer's disease, tumor classification/segmentation) using MRI, CT, and PET images, including EEG signals.

AZIZ-UL-REHMAN received the M.Sc. and M.Phil. Diploma degrees in applied physics from UET Lahore, Pakistan, in 2003 and 2005, respectively, the M.S. degree in medical physics from Pakistan Institute of Engineering and Applied Sciences (PIEAS), in 2007, and the Ph.D. degree from Macquarie University, Sydney, NSW, Australia, in 2018. He is currently an Assistant Professor/Senior Scientist with the Agriculture and Biophotonics Division, National Institute of Lasers and Optronics College, PIEAS. His research interests include light tissue interaction, optical diagnosis, hyperspectral auto-fluorescence imaging of biological tissues, unsupervised unmixing, photodiagnosis and photodynamic therapy, Raman spectroscopy of biomolecules, IAD methods, deep-UV light sources design and implementation in optical diagnosis, radiology, and radiotherapy.

LAL HUSSAIN received the M.S. degree (Hons.) in communication and networks from Iqra University, Islamabad, Pakistan, in 2012, and the Ph.D. degree from the Department of Computer Science and Information Technology, The University of Azad Jammu and Kashmir, Muzaffarabad, Pakistan, in February 2016. He was a Visiting Ph.D. Researcher at Lancaster University, U.K., for six months under the HEC International Research Initiative Program and worked under the supervision of Dr. Aneta Stefanovska, Biomedical Physics, Physics Department, Lancaster University, from 2014 to 2015. He recently completed a one-year Postdoctoral Fellowship from the Montefiore Medical Center and the Albert Einstein College of Medicine, USA, under the supervision of Dr. Tim Q. Duong, a Professor and the Vice Chair of MRI Research. He was also with the Duong Laboratory, Stony Brook University, USA, in different on-going projects with Dr. Duong, from January 2020 to March 2020. He is currently an Assistant Professor with the Department of Computer Science and Information Technology, The University of Azad Jammu and Kashmir. He is the author of more than 50 publications in highly reputed peer-reviewed and impact fact journals as a principal author. He completed various funded projects as PI and Co-PI from Ignite, ICT Pakistan, the University of Jeddah, and Saudi Electronic University, Saudi Arabia. He presented various talks in Pakistan, U.K., Peru, and USA. His research interests include developing and optimizing AI tools, including machine learning, deep learning, neural networks algorithms, feature extraction and selection methods, information-theoretic methods, time-frequency representation methods, cross-frequency coupling to predict the disease severity, progression, survival, and recurrence, biomedical signal and image processing problems, including prostate cancer, breast cancer, lung cancer, brain tumor, covid-19 lung infection with different modalities (MRI, CT, and X-Ray), and brain dynamics and diseases (autism spectrum disorder (ASD) and attention-deficit/hyperactivity disorder (ADHD), Alzheimer's Disease). Recently, he was ranked in 1% top world scientists list of 2021 by Elsevier based on research records.

TOUSEEF SADIQ (Member, IEEE) received the B.E. degree in computer engineering from Bahria University Islamabad, Pakistan, and the M.S. degree in communications and computer networks engineering from the Polytechnic University of Turin, Italy, on a fully-funded scholarship. He is currently a Research Fellow with the University of Agder, Norway, and working with the Centre for Artificial Intelligence Research (CAIR). He has contributed significantly to the academic community as an author and co-author of multiple publications in respected journals and conferences, furthering advancements in AI and its practical applications. His research interests encompass a broad range of topics within artificial intelligence, including machine learning, computer vision, and deep multimodal learning, with a focus on their applications in smart cities.

SYED TAIMOOR HUSSAIN SHAH is currently an Early-Stage Researcher in the PARENT project, funded by European Union's Horizon 2020 initiative, based at Politecnico di Torino, Italy. His work focuses on artificial intelligence, machine learning, and computer vision, with applications in biomedical imaging, signal processing, hyperspectral imaging, and other related diverse problems.

ADIL ASLAM MIR received the Ph.D. degree from Ankara Yıldırım Beyazıt University, Türkiye, in 2022. Currently, he is an Assistant Professor with the Department of Computer Science and Information Technology, The University of Azad Jammu and Kashmir. His research interests include machine learning-based decision support systems (DSSs), data mining, and artificial intelligence.

MUHAMMAD AMIN NADIM received the M.S. degree in computer science from the University of South Asia, Lahore, Pakistan, in 2017. He is currently pursuing the Ph.D. degree with the National Doctorate Program in Learning Sciences and Digital Technologies, Università Telematica Pegaso and Università degli Studi di Foggia, combined universities in Italy. His research interests include developing and optimizing AI tools, including machine learning, deep learning, neural network algorithms, and feature extraction and selection methods to predict disease severity, progression, survival, and recurrence. Furthermore, his areas of interest are different aspects of artificial intelligence, including generative AI and education, AI and E-learning, machine learning, data science, data analytics, predictive analysis, and the role of AI ethics in education. He is recently a member of the Association for Computing Machinery (ACM), USA; the Coalition of Schools Educating Mindfully (COSEM), USA; the International Society for Professional Innovation Management (ISPIM); and Austrian Society of Artificial Intelligence (ASAI). He presented various talks in Pakistan, Italy, Spain, India, and Türkiye. He currently performs tasks as a Reviewer of *European Journal of Education* and *Canadian Journal of Learning and Technology*.

DARNELL K. ADRIAN WILLIAMS is currently pursuing the M.D.-Ph.D. degree and future physician-scientist with a demonstrated passion for research, leadership, and advocacy. His research interests center around using computational methods to better understand and treat neurological problems. He is particularly interested in identifying and combating healthcare disparities, neuroscience, psychiatric diseases, biomedical imaging, big data, AI/ML, and biotechnology/startups. Previously, he worked in the labs of Jeremy Gunawardena at Harvard Medical School's Systems Biology Department and Conor Liston, Weill Cornell Medical College, where he studied transcranial magnetic stimulation (TMS) as a treatment for treatment-resistant depression using neuroimaging and machine learning. He joined the Coen-Cagli laboratory at Einstein in 2024.
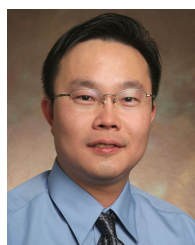
TIM Q. DUONG received the Ph.D. degree in 1998. He is a Professor and a Vice Chair of Research with the Department of Radiology, Albert Einstein College of Medicine and Montefiore Health System. He also serves as the Associate Director of Integrative Imaging and Data Science at the Center for Health and Data Innovation and as the Director of the Biomedical Imaging Ph.D. Program. His research focuses on developing and applying advanced medical imaging techniques, particularly MRI, to study health and disease, aiming at early detection, accurate diagnosis, and evaluation of disease progression and treatment responses. He has authored over 310 publications and has been cited more than 19,000 times, reflecting his significant contributions to the field. He has since been actively involved in advancing biomedical imaging research and education.

QURAT-UL-AIN CHAUDHARY received the bachelor's and master's degrees in computer science from The University of Azad Jammu and Kashmir. She is currently pursuing the Ph.D. degree with the Department of Computer and Information Sciences, Pakistan Institute of Engineering and Applied Sciences. Her research interests include medical image processing, machine learning, and deep learning.

ASRAR AHMAD received the M.Sc. degree in physics from the GCS, Lahore, the M.S. degree in medical physics from Pakistan Institute of Engineering and Applied Sciences (PIEAS), and the Ph.D. degree in medical radiation physics from Dresden University of Technology, Dresden, Germany. While working on his Ph.D. project, he also gained hands-on experience in both photon and proton therapies at the University Clinic Dresden.

NATASHA HABIB received the bachelor's degree in physics from Pakistan Institute of Engineering and Applied Sciences (PIEAS). Her academic journey reflects a strong commitment to leveraging advanced technologies for medical applications, making her a promising early-career researcher in the scientific community. Her research interests include artificial intelligence and medical physics, where she has actively contributed to exploring innovative solutions at the intersection of these fields.

SYED ADIL HUSSAIN SHAH is currently pursuing the Ph.D. degree with Politecnico di Torino, Turin, Italy. He is also an IT Researcher with GPI SpA, Trento, Italy. His field of expertise is related to machine vision, biomedical imaging, signal processing, and intelligence system development.

• • •